

# Regularized MFS-Based Boundary Identification in Two-Dimensional Helmholtz-Type Equations

Liviu Marin<sup>1</sup> and Andreas Karageorghis<sup>2</sup>

**Abstract:** We study the stable numerical identification of an unknown portion of the boundary on which a given boundary condition is provided and additional Cauchy data are given on the remaining known portion of the boundary of a two-dimensional domain for problems governed by either the Helmholtz or the modified Helmholtz equation. This inverse geometric problem is solved using the method of fundamental solutions (MFS) in conjunction with the Tikhonov regularization method. The optimal value for the regularization parameter is chosen according to Hansen's L-curve criterion. The stability, convergence, accuracy and efficiency of the proposed method are investigated by considering several examples.

**Keywords:** Helmholtz-Type Equations; Inverse Geometric Problem; Method of Fundamental Solutions (MFS); Regularization.

## 1 Introduction

In *direct problems* in mechanics, the goal is to determine the response of a system when the governing system of partial differential equations, the initial and boundary conditions for the primary and/or secondary fields, the material properties and the geometry of the domain occupied by the material under investigation are all known. The existence and uniqueness of the solution to such problems have been well established. If, however, at least one of the above data is partially or entirely missing, this yields an *inverse problem*. It is well known that such problems are in general unstable, in the sense that small measurement errors in the input data may significantly amplify the errors in the solution, see e.g. Hadamard (1923).

An important class of inverse problems in mechanics is represented by *inverse geometric problems* which can be divided into the following categories: (i) shape and

---

<sup>1</sup> Institute of Solid Mechanics, Romanian Academy, 15 Constantin Mille, Sector 1, P.O. Box 1-863, 010141 Bucharest, Romania. E-mails: [marin.liviu@gmail.com](mailto:marin.liviu@gmail.com); [liviu@imsar.bu.edu.ro](mailto:liviu@imsar.bu.edu.ro)

<sup>2</sup> Department of Mathematics and Statistics, University of Cyprus, P.O. Box 20537, 1678 Nicosia, Cyprus. E-mail: [andreask@ucy.ac.cy](mailto:andreask@ucy.ac.cy)

design optimization; (ii) identification of defects, e.g. cavities, inclusions, cracks; and (iii) identification of an unknown part of the boundary. For problems belonging to the last category, both Dirichlet and Neumann data, i.e. Cauchy data, can be measured on an accessible and known part of the boundary of the solution domain, whilst either a Dirichlet, Neumann or Robin-type condition is prescribed on the remaining, inaccessible and unknown, part of the boundary. In such problems, the goal is to reconstruct the unknown part of the boundary from the available boundary conditions.

Most of the studies available in the literature which investigate the boundary identification (reconstruction) problem deal with the Laplace equation. Aparicio and Pidcock (1996) analysed the problem of determining a part of the boundary of a domain, where a potential satisfies the Laplace equation, and proposed two methods to solve this problem, provided that the potential is monotonic along the unknown boundary. The stability of determining a portion of the boundary, which encloses a two-dimensional bounded domain where the Laplace equation is satisfied, from Cauchy data was studied by Beretta and Vessela (1998). Various conditional stability estimates for this problem, according to *a priori* assumptions on the regularity of the unknown sub-boundaries, were provided by Bukhgeim, Cheng and Yamamoto (1999). Hsieh and Kassab (1986) proposed a general numerical method to determine an unknown boundary for heat conduction problems which is independent of the type of condition imposed on the unknown boundary. Huang and Chao (1997) investigated a steady-state shape identification problem by using both the Levenberg-Marquardt algorithm and the conjugate gradient method. Their work was later extended by Huang and Tsai (1998) to a transient inverse geometric problem in identifying the irregular boundary configurations from external measurements using the boundary element method (BEM). Park and Ku (2001) considered the inverse problem of identifying the boundary shape of a domain from boundary temperature measurements, when the temperature is dominated by natural convection. Lesnic, Berger and Martin (2002) determined the boundary in potential corrosion damage from Cauchy data available on the known portion of the boundary by employing a regularized BEM minimization technique. Their method was also extended to the Lamé system of linear elasticity and the Helmholtz equation by Marin and Lesnic (2003), and Marin (2006), respectively.

The method of fundamental solutions (MFS) is a meshless boundary collocation method which is applicable to boundary value problems for which a fundamental solution of the operator in the governing equation is known. Although the ideas behind the method had been around for a number of years, it was introduced as a numerical method in the late 70's by Mathon and Johnston (1977). In recent years the MFS has been used for the numerical solution of a large variety of phys-

ical problems, see e.g. Tsangaris, Smyrlis and Karageorghis (2004); Alves and Antunes (2005); Reutskiy (2005); Young, Tsai, Lin and Chen (2006); Godinho, Tadeu and Amado Mendes (2007); Chen, Kao and Chen (1995). For a comprehensive application of the MFS to various problems, we refer the reader to the survey papers Fairweather and Karageorghis (1998); Golberg and Chen (1999); Fairweather, Karageorghis and Martin (2003) and Cho, Golberg, Muleshkov and Li (2004). The main reason for the popularity of the method is the ease with which it can be implemented, especially for problems in complex geometries and three-dimensional domains.

Predictably, this ease of implementation of the method for problems with complex boundaries has attracted the attention of several researchers in the area of inverse problems and as a result, the MFS has been used extensively for the numerical solution of such problems; for a brief review see Marin, Karageorghis and Lesnic (2009). In particular, recently, the MFS has been successfully applied to solving inverse problems associated with the heat equation [Hon and Wei (2004); Hon and Wei (2005); Dong, Sun and Meng (2007); Ling and Takeuchi (2008); Marin (2008); Shigeta and Young (2009)], linear elasticity [Marin and Lesnic (2004); Marin (2005a); Fam and Rashed (2009)], steady-state heat conduction in functionally graded materials (FGMs) [Marin (2005b)], Helmholtz-type equations [Marin and Lesnic (2005a); Marin (2005c); Jin and Zheng (2006)], the biharmonic equation [Marin and Lesnic (2005b); Zeb, Ingham and Lesnic (2008)], source reconstruction in heat conduction problems [Jin and Marin (2007); Yan, Fu and Yang (2008)], Stokes problems [Chen, Young, Tsai and Murugesan (2005)], etc.

The first attempt to solve an inverse geometric problem by a meshless method was carried out by Hon and Wu (2000), where radial basis functions were used to approximate the solution. The MFS was, apparently, used for the first time for the solution of an inverse boundary determination problem in Mera and Lesnic (2005), where the authors solved the corresponding inverse problem associated with the three-dimensional Laplace equation arising in potential corrosion damage. In Hon and Li (2008), the MFS was applied to one- and two-dimensional inverse boundary determination heat conduction problems. Zeb, Ingham and Lesnic (2008) applied the MFS, without any physical constraints, to the solution of an inverse boundary determination problem associated with the two-dimensional biharmonic equation. Recently, a combined MFS-Tikhonov regularization method was introduced to reconstruct the inaccessible and unknown part of the boundary of the domain from Cauchy data on the remaining accessible portion of the boundary for two-dimensional harmonic problems, FGMs and isotropic linear elastic materials, see Marin, Karageorghis and Lesnic (2009), Marin (2009a) and Marin (2009b), respectively.

To the best of our knowledge, the application of the MFS to two-dimensional inverse geometric problems governed by either the Helmholtz or the modified Helmholtz equation, has not yet been investigated. More specifically, we try to identify, in a stable manner, the shape of an inaccessible and unknown part of the boundary of the solution domain, from a prescribed boundary condition on this portion of the boundary and Cauchy data available on the remaining, accessible and known part of the boundary. This inverse problem is solved using the MFS, in conjunction with the Tikhonov first-order regularization method, i.e. by extending the method proposed by Marin, Karageorghis and Lesnic (2009), Marin (2009a) and Marin (2009b) to problems governed by the two-dimensional Helmholtz and modified Helmholtz equations. The optimal value of the regularization parameter is chosen according to Hansen's L-curve criterion.

## 2 Mathematical formulation

Helmholtz-type equations arise naturally in many physical applications such as the vibration of a structure, the acoustic cavity problem, the radiation wave, the scattering of a wave and the heat conduction in fins. In this work, in order to refer to a specific physical problem, we shall consider Helmholtz problems in the context of heat transfer problems, see e.g. Kraus, Aziz and Welty (2001).

We therefore assume that the temperature field,  $u(\mathbf{x})$ , satisfies the Helmholtz or the modified Helmholtz equation in an open bounded domain  $\Omega \subset \mathbb{R}^2$ , namely

$$\mathcal{L}u(\mathbf{x}) \equiv (\Delta \pm \kappa^2)u(\mathbf{x}) = 0, \quad \mathbf{x} = (x_1, x_2) \in \Omega, \quad (1)$$

where  $\kappa > 0$ , while the plus and minus signs correspond to the Helmholtz and the modified Helmholtz equations, respectively. Moreover, we assume that the domain  $\Omega$  is bounded by a smooth or a piecewise smooth curve  $\partial\Omega$ , such that  $\partial\Omega = \partial\Omega_1 \cup \partial\Omega_2$ , where  $\partial\Omega_1 \neq \emptyset$ ,  $\partial\Omega_2 \neq \emptyset$  and  $\partial\Omega_1 \cap \partial\Omega_2 = \emptyset$ . For example, when  $\mathcal{L} \equiv \Delta - \kappa^2$ , the partial differential equation (1) models the heat conduction in a fin where  $u$  is the dimensionless local fin temperature,  $\kappa^2 = h/(k \delta_f)$ ,  $h$  is the surface heat transfer coefficient [ $\text{W}/(\text{m}^2\text{K})$ ],  $k$  is the thermal conductivity of the fin [ $\text{W}/(\text{mK})$ ] and  $\delta_f$  is the half-fin thickness [m].

Let  $\mathbf{n}(\mathbf{x})$  be the unit outward normal vector to the boundary  $\partial\Omega$  and  $q(\mathbf{x}) \equiv \nabla u(\mathbf{x}) \cdot \mathbf{n}(\mathbf{x})$  be the normal heat flux at a point  $\mathbf{x} \in \partial\Omega$ . In the direct problem formulation, the knowledge of the constant  $\kappa$ , the location, shape and size of the entire boundary  $\partial\Omega$ , the temperature and/or the normal heat flux on the entire boundary  $\partial\Omega$  gives the corresponding Dirichlet, Neumann, or mixed boundary conditions which enable one to determine the unknown boundary conditions, as well as the temperature distribution in the solution domain. A different and more interesting situation arises

when a part of the boundary, say  $\partial\Omega_2$ , is unknown, while some additional information is supplied on the remaining part of the boundary  $\partial\Omega_1 = \partial\Omega \setminus \partial\Omega_2$ . More precisely, we consider the following inverse geometric problem for two-dimensional Helmholtz-type equations:

Determine the boundary  $\partial\Omega_2 \subset \partial\Omega$ ,  $\partial\Omega_2 \neq \emptyset$ , such that the temperature  $u$  satisfies the Helmholtz (or modified Helmholtz) equation (1), both temperature and flux conditions, i.e. Cauchy data, are given on the known part of the boundary, and either a Dirichlet, Neumann or Robin boundary condition is prescribed on  $\partial\Omega_2$ , namely

$$\mathcal{L}u(\mathbf{x}) \equiv (\Delta \pm \kappa^2)u(\mathbf{x}) = 0, \quad \mathbf{x} \in \Omega, \quad (2a)$$

$$u(\mathbf{x}) = \tilde{u}(\mathbf{x}), \quad \mathbf{x} \in \partial\Omega_1, \quad (2b)$$

$$q(\mathbf{x}) = \tilde{q}(\mathbf{x}), \quad \mathbf{x} \in \partial\Omega_1, \quad (2c)$$

$$\alpha_u u(\mathbf{x}) + \alpha_q q(\mathbf{x}) = \tilde{f}(\mathbf{x}), \alpha_q, \quad \mathbf{x} \in \partial\Omega_2. \quad (2d)$$

Here  $\alpha_u, \alpha_q \in \mathbb{R}$ , while  $\tilde{u}$ ,  $\tilde{q}$  and  $\tilde{f}$  are prescribed Dirichlet, Neumann and Robin boundary conditions, respectively. It should be noted that, in Eq. (2d), the cases when  $\alpha_u = 1$  and  $\alpha_q = 0$ , and  $\alpha_u = 0$  and  $\alpha_q = 1$  correspond to given Dirichlet and Neumann boundary conditions on  $\partial\Omega_2$ , respectively, while the condition  $\alpha_u \alpha_q \neq 0$  is associated with a prescribed Robin boundary condition on  $\partial\Omega_2$ .

In addition, we assume that the known boundary  $\partial\Omega_1$  is the graph of a known Lipschitz function  $\phi_1 : [-r, r] \rightarrow [0, \infty)$ , whilst the unknown boundary  $\partial\Omega_2$  is the graph of an unknown Lipschitz function  $\phi_2 : [-r, r] \rightarrow \mathbb{R}$ , where  $\phi_1(x) > \phi_2(x)$  for all  $x \in (-r, r)$ . Moreover, both the known and unknown boundaries intersect the  $x_1$ -coordinate axis at the points  $(\pm r, 0)$ , see e.g. Fig. 1.

This inverse geometric problem is considerably more difficult to solve than the direct problem, both analytically and numerically, since the solution does not satisfy the general conditions of well-posedness. Although the problem may have a unique solution, it is well-known that this solution is unstable with respect to small perturbations to the data on  $\partial\Omega_1$ , see e.g. Hadamard (1923). Thus the problem is ill-posed and we cannot use a direct approach, such as the least-squares method, in order to solve the system of linear equations which arises from the discretization of the partial differential equations (2a) and the boundary conditions (2b) – (2d).

### 3 Method of fundamental solutions

#### 3.1 Boundary discretization

The boundary  $\partial\Omega$  of the solution domain  $\Omega$  is discretized by selecting  $N_1$  boundary points  $\mathbf{z}^{(i)}$ ,  $i = 1, \dots, N_1$ , on the known boundary  $\partial\Omega_1$  and  $N_2$  boundary points

$\mathbf{z}^{(N_1+i)}$ ,  $i = 1, \dots, N_2$ , on the unknown boundary  $\partial\Omega_2$ , such that  $N = N_1 + N_2$ . Consequently, the boundary  $\partial\Omega$  is approximated by

$$\partial\Omega \approx \partial\tilde{\Omega} = \bigcup_{i=1}^{N_1+N_2} \Gamma^{(i)}, \quad \text{where } \Gamma^{(i)} = [\mathbf{z}^{(i)}, \mathbf{z}^{(i+1)}], \quad i = 1, \dots, N_1 + N_2, \quad (3)$$

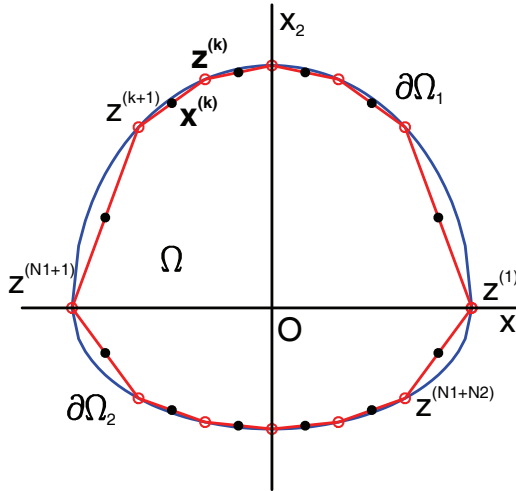


Figure 1: Geometry and boundary discretization of the problem.

with the convention  $\mathbf{z}^{(N_1+N_2+1)} = \mathbf{z}^{(1)}$ . As a direct consequence of the discretization given by Eq. (3), the known and unknown boundaries  $\partial\Omega_1$  and  $\partial\Omega_2$  are approximated by

$$\partial\Omega_1 \approx \partial\tilde{\Omega}_1 = \bigcup_{i=1}^{N_1} \Gamma^{(i)} \quad \text{and} \quad \partial\Omega_2 \approx \partial\tilde{\Omega}_2 = \bigcup_{i=N_1+1}^{N_1+N_2} \Gamma^{(i)}, \quad \text{respectively.} \quad (4)$$

Further, we take the MFS boundary collocation points to be the midpoints  $\mathbf{x}^{(i)}$ ,  $i = 1, \dots, N_1 + N_2$ , of each segment  $\Gamma^{(i)}$ ,  $i = 1, \dots, N_1 + N_2$ , namely

$$\mathbf{x}^{(i)} = \frac{1}{2} (\mathbf{z}^{(i)} + \mathbf{z}^{(i+1)}) = \mathbf{x}^{(i)} (\mathbf{z}^{(i)}, \mathbf{z}^{(i+1)}), \quad i = 1, \dots, N_1 + N_2. \quad (5)$$

In this way, the outward unit normal vector  $\mathbf{n}$  to the approximate boundary  $\partial\tilde{\Omega}$  at the MFS boundary collocation points is given by

$$\mathbf{n}(\mathbf{x}^{(i)}) = \frac{1}{\|\mathbf{z}^{(i+1)} - \mathbf{z}^{(i)}\|} \left( z_2^{(i+1)} - z_2^{(i)}, -z_1^{(i+1)} + z_1^{(i)} \right) = \mathbf{n}^{(i)} (\mathbf{z}^{(i)}, \mathbf{z}^{(i+1)}), \quad (6)$$

$$i = 1, \dots, N_1 + N_2.$$

The boundary points  $\mathbf{z}^{(i)}$ ,  $i = 1, \dots, N_1 + N_2$ , are chosen so that their  $x_1$ -components are uniformly distributed on the segment  $[-r, r]$ , while the  $x_2$ -components are expressed as functions of the corresponding  $x_1$ -components. More specifically, we define the boundary points  $\mathbf{z}^{(i)}$ ,  $i = 1, \dots, N_1 + N_2$ , in the following way, see also Fig. 1,

$$\mathbf{z}^{(i)} = \left( z_1^{(i)}, z_2^{(i)} \right), \quad i = 1, \dots, N_1 + N_2, \quad (7a)$$

$$z_1^{(i)} = r \left( 1 - 2 \frac{i-1}{N_1} \right), \quad z_2^{(i)} = \phi_1(z_1^{(i)}), \quad i = 1, \dots, N_1, \quad (7b)$$

$$z_1^{(N_1+i)} = -r \left( 1 - 2 \frac{i-1}{N_2} \right), \quad z_2^{(N_1+i)} = \phi_2(z_1^{(N_1+i)}), \quad i = 1, \dots, N_2, \quad (7c)$$

$$\mathbf{z}^{(1)} = (r, 0), \quad \mathbf{z}^{(N_1+1)} = (-r, 0). \quad (7d)$$

Consequently, the MFS boundary collocation points  $\mathbf{x}^{(i)}$ ,  $i = 1, \dots, N_1 + N_2$ , are given by

$$\mathbf{x}^{(i)} = \left( x_1^{(i)}, x_2^{(i)} \right), \quad i = 1, \dots, N_1 + N_2, \quad (8a)$$

$$x_1^{(i)} = r \left( 1 - \frac{2i-1}{N_1} \right), \quad x_2^{(i)} = \frac{1}{2} \left( z_2^{(i)} + z_2^{(i+1)} \right), \quad i = 1, \dots, N_1, \quad (8b)$$

$$x_1^{(N_1+i)} = -r \left( 1 - \frac{2i-1}{N_2} \right), \quad x_2^{(N_1+i)} = \frac{1}{2} \left( z_2^{(N_1+i)} + z_2^{(N_1+i+1)} \right), \quad i = 1, \dots, N_2. \quad (8c)$$

From Eqs. (7) and (8), it follows that the unknown boundary  $\partial\Omega_2$  is completely determined by the unknown vector  $\mathbf{z} = \left[ z_2^{(N_1+2)}, \dots, z_2^{(N_1+N_2)} \right]^T \in \mathbb{R}^{N_2-1}$ .

### 3.2 MFS approximation

The fundamental solutions of the Helmholtz ( $G_H$ ) and the modified Helmholtz ( $G_{MH}$ ) equations in two-dimensions are given by, see e.g. Fairweather and Karageorghis (1998), and Marin and Lesnic (2005a)

$$G_H(\mathbf{x}, \xi) = \frac{i}{4} H_0^{(1)}(\kappa \|\mathbf{x} - \xi\|), \quad \mathbf{x} \in \bar{\Omega}, \quad \xi \in \mathbb{R}^2 \setminus \bar{\Omega}, \quad (9a)$$

and

$$G_{MH}(\mathbf{x}, \xi) = \frac{1}{2\pi} K_0(\kappa \|\mathbf{x} - \xi\|), \quad \mathbf{x} \in \bar{\Omega}, \quad \xi \in \mathbb{R}^2 \setminus \bar{\Omega}, \quad (9b)$$

respectively. Here  $i = \sqrt{-1}$ ,  $\xi$  is a singularity (or source point),  $H_0^{(1)}$  is the Hankel function of the first kind of order zero and  $K_0$  is the modified Bessel function of the second kind of order zero.

In the MFS, we approximate the temperature in the solution domain by a linear combination of fundamental solutions with respect to  $M$  singularities  $\xi^{(j)}$ ,  $j = 1, \dots, M$ , in the form

$$u(\mathbf{x}) \approx u_M(\mathbf{c}, \xi; \mathbf{x}) = \sum_{j=1}^M c_j G(\mathbf{x}, \xi^{(j)}), \quad \mathbf{x} \in \bar{\Omega}, \quad (10)$$

where  $\mathbf{c} = [c_1, \dots, c_M]^T$  and  $\xi \in \mathbb{R}^{2M}$  is a vector containing the coordinates of the singularities  $\xi^{(j)}$ ,  $j = 1, \dots, M$ . Taking into account the definitions of the normal heat flux and the fundamental solutions for the Helmholtz and the modified Helmholtz equations (9), the normal heat flux, through a curve defined by the outward unit normal vector  $\mathbf{n}(\mathbf{x})$ , can be approximated on the boundary  $\partial\Omega$  by

$$q(\mathbf{x}) \approx q_M(\mathbf{c}, \xi; \mathbf{x}) = \sum_{j=1}^M c_j H(\mathbf{x}, \xi^{(j)}), \quad \mathbf{x} \in \partial\Omega. \quad (11)$$

Here  $H(\mathbf{x}, \xi) = \nabla_{\mathbf{x}} G(\mathbf{x}, \xi) \cdot \mathbf{n}(\mathbf{x})$ , and  $H = H_H$  in the case of the Helmholtz equation and  $H = H_{MH}$  in the case of the modified Helmholtz equation, where

$$H_H(\mathbf{x}, \xi) = -\frac{i\kappa}{4} H_1^{(1)}(\kappa \|\mathbf{x} - \xi\|) \left[ \frac{\mathbf{x} - \xi}{\|\mathbf{x} - \xi\|} \cdot \mathbf{n}(\mathbf{x}) \right], \quad \mathbf{x} \in \bar{\Omega}, \quad \xi \in \mathbb{R}^2 \setminus \bar{\Omega}, \quad (12a)$$

and

$$H_{MH}(\mathbf{x}, \xi) = -\frac{\kappa}{2\pi} K_1(\kappa \|\mathbf{x} - \xi\|) \left[ \frac{\mathbf{x} - \xi}{\|\mathbf{x} - \xi\|} \cdot \mathbf{n}(\mathbf{x}) \right], \quad \mathbf{x} \in \bar{\Omega}, \quad \xi \in \mathbb{R}^2 \setminus \bar{\Omega}, \quad (12b)$$

respectively. In Eqs. (12a) and (12b),  $H_1^{(1)}$  is the Hankel function of the first kind of order one and  $K_1$  the modified Bessel function of second kind of order one.

From the MFS approximations (10) and (11), boundary conditions (2b) – (2d) yield

$$\sum_{j=1}^M G(\mathbf{x}^{(i)}, \xi^{(j)}) c_j = \tilde{u}(\mathbf{x}^{(i)}), \quad i = 1, \dots, N_1, \quad (\partial\Omega_1) \quad (13a)$$

$$\sum_{j=1}^M H(\mathbf{x}^{(i)}, \xi^{(j)}) c_j = \tilde{q}(\mathbf{x}^{(i)}), \quad i = 1, \dots, N_1, \quad (\partial\Omega_1) \quad (13b)$$

$$\sum_{j=1}^M \left[ \alpha_u G(\mathbf{x}^{(i)}, \xi^{(j)}) + \alpha_q H(\mathbf{x}^{(i)}, \xi^{(j)}) \right] c_j = \tilde{f}(\mathbf{x}^{(i)}), \quad (\partial\Omega_2) \quad (13c)$$

$$i = N_1 + 1, \dots, N_1 + N_2.$$

Eqs. (13a) – (13c) represent a system of  $2N_1 + N_2$  nonlinear algebraic equations with  $M + N_2 - 1$  unknowns, namely the MFS coefficients  $\mathbf{c} = [c_1, \dots, c_M]^T \in \mathbb{R}^M$  and the  $x_2$ -coordinates  $\mathbf{z} = [z_2^{(N_1+2)}, \dots, z_2^{(N_1+N_2)}]^T \in \mathbb{R}^{N_2-1}$  of the boundary points that determine the unknown boundary  $\partial\Omega_2$ . It should be noted that in order to uniquely determine the solution  $(\mathbf{c}, \mathbf{z}) \in \mathbb{R}^M \times \mathbb{R}^{N_2-1}$  of the system of nonlinear algebraic equations (13a) – (13c), the number  $N_1$  of boundary collocation points on the known boundary  $\partial\Omega_1$  and the number  $M$  of singularities must satisfy the inequality  $M - 1 \leq 2N_1$ . Further, the system of nonlinear algebraic equations (13a) – (13c) cannot be solved by direct methods, such as the least-squares method, since such an approach would produce a highly unstable solution.

### 3.3 MFS boundary collocation points and singularities

In order to implement the MFS, the location of the singularities has to be determined and this is usually achieved by considering either the static or the dynamic approach. In the static approach, the singularities are kept fixed throughout the solution process, while in the dynamic approach, the singularities and the unknown coefficients are determined simultaneously during the solution process, see Fairweather and Karageorghis (1998). In the latter approach which is computationally much more expensive, the uniqueness of the solution is not always guaranteed. Thus the dynamic approach transforms the inverse geometric problem into a nonlinear ill-posed problem. We have therefore decided to employ the static approach with the singularities,  $\xi^{(j)}$ ,  $j = 1, \dots, M$ , located on the boundary,  $\partial\Omega_S$ , of a disk of radius  $R_S$  and centered at the origin, defined by  $\Omega_S = \{ \mathbf{x} = (x_1, x_2) \mid x_1^2 + x_2^2 < R_S^2 \}$ , that encloses the solution domain, as well as its boundary, i.e.  $\bar{\Omega} \subset \Omega_S$ .

## 4 Description of the algorithm

In this section, we present a numerical scheme for the stable solution of the system of nonlinear algebraic equations (13a) – (13c), as well as details regarding the numerical implementation of the proposed method.

### 4.1 Tikhonov regularization method

Several regularization techniques used for the stable solution of systems of linear and nonlinear algebraic equations are available in the literature, such as the Singular Value Decomposition (SVD) [Hansen (1998)], the Tikhonov regularization method

[Tikhonov and Arsenin (1986)] and various iterative methods [Kunisch and Zou (1998)]. Recently, Liu (2008a) proposed a new and robust numerical technique for the stable solution of ill-posed systems of linear algebraic equations, namely the Fictitious Time Integration Method (FTIM). This method consists of introducing a fictitious time variable that plays the role of a regularization parameter, while its filtering effect is better than that of the Tikhonov and exponential filters. The FTIM was successfully applied to solving inverse vibration problems [Liu (2008b); Liu (2008c); Liu, Chang, Chang and Chen (2008)], nonlinear complementarity problems [Liu (2008d)], large systems of nonlinear algebraic equations [Liu and Atluri (2008a)], boundary value problems for elliptic partial differential equations [Liu (2008e)] and inverse Sturm-Liouville problems [Liu and Atluri (2008b)]. Liu and Atluri (2009) have recently shown that, when applied to solving an ill-posed system of linear equations, the general FTIM may be viewed as a special case of the Tikhonov regularization method.

The inverse geometric problem investigated in this paper is solved, in a stable manner, by minimizing the following Tikhonov regularization functional, see Tikhonov and Arsenin (1986),

$$\mathcal{F}_\lambda(\cdot, \cdot) : \mathbb{R}^M \times \mathbb{R}^{N_2-1} \longrightarrow [0, \infty), \quad \mathcal{F}_\lambda(\mathbf{c}, \mathbf{z}) = \mathcal{F}_{LS}(\mathbf{c}, \mathbf{z}) + \mathcal{R}_\lambda(\mathbf{z}), \quad (14)$$

where  $\mathcal{F}_{LS}$  is the least-squares functional associated with the inverse geometric problem investigated in this study,  $\mathcal{R}_\lambda$  is the regularization term to be specified and  $\lambda > 0$  is the regularization parameter to be prescribed.

The least-squares functional,  $\mathcal{F}_{LS}$ , in Eq. (14) is given by

$$\begin{aligned} \mathcal{F}_{LS}(\cdot, \cdot) : \mathbb{R}^M \times \mathbb{R}^{N_2-1} &\longrightarrow [0, \infty), \\ \mathcal{F}_{LS}(\mathbf{c}, \mathbf{z}) &= \frac{1}{2} \sum_{i=1}^{N_1} \left\{ \left[ \mathcal{F}_1(\mathbf{c}, \xi; \mathbf{x}^{(i)}) \right]^2 + \left[ \mathcal{F}_2(\mathbf{c}, \xi; \mathbf{x}^{(i)}) \right]^2 \right\} \\ &+ \frac{1}{2} \sum_{i=N_1+1}^{N_1+N_2} \left[ \mathcal{F}_3(\mathbf{c}, \xi; \mathbf{x}^{(i)}) \right]^2, \end{aligned} \quad (15)$$

where

$$\mathcal{F}_1(\mathbf{c}, \xi; \mathbf{x}^{(i)}) = \tilde{\mathbf{u}}(\mathbf{x}^{(i)}) - \mathbf{u}_M(\mathbf{c}, \xi; \mathbf{x}^{(i)}), \quad i = 1, \dots, N_1, \quad (16a)$$

$$\mathcal{F}_2(\mathbf{c}, \xi; \mathbf{x}^{(i)}) = \tilde{\mathbf{q}}(\mathbf{x}^{(i)}) - \mathbf{q}_M(\mathbf{c}, \xi; \mathbf{x}^{(i)}), \quad i = 1, \dots, N_1, \quad (16b)$$

$$\mathcal{F}_3(\mathbf{c}, \xi; \mathbf{x}^{(i)}) = \tilde{\mathbf{f}}(\mathbf{x}^{(i)}) - [\alpha_u \mathbf{u}_M(\mathbf{c}, \xi; \mathbf{x}^{(i)}) + \alpha_q \mathbf{q}_M(\mathbf{c}, \xi; \mathbf{x}^{(i)})], \quad (16c)$$

$$i = N_1 + 1, \dots, N_1 + N_2.$$

The regularization term,  $\mathcal{R}_\lambda$ , in Eq. (14) is chosen to be the Tikhonov first-order regularization term, namely

$$\mathcal{R}_\lambda(\cdot) : \mathbb{R}^{N_2-1} \longrightarrow [0, \infty), \quad \mathcal{R}_\lambda(\mathbf{z}) = \lambda \|\mathbf{z}'\|^2. \quad (17)$$

Here  $\mathbf{z}' = \left[ z_2^{(N_1+2)} - z_2^{(N_1+1)}, \dots, z_2^{(N_1+N_2+1)} - z_2^{(N_1+N_2)} \right]^T$  denotes an approximation to the first-order derivative of the function  $\phi_2$ , keeping in mind that  $z_1^{(i+1)} - z_1^{(i)}$ ,  $i = N_1, \dots, N_1 + N_2$ , is constant.

It should be emphasized that the zeroth-order Tikhonov regularization procedure, which is based on penalizing the norm of the solution, i.e.  $\mathcal{R}_\lambda(\mathbf{z}) = \lambda \|\mathbf{z}\|^2$  in Eq. (14), rather than its derivative, i.e.  $\mathcal{R}_\lambda(\mathbf{z}) = \lambda \|\mathbf{z}'\|^2$ , did not produce satisfactorily accurate and stable results for the unknown boundary  $\partial\Omega_2$ . This observation is consistent with the results obtained by Peneau, Jarny and Sarda (1996), Lesnic, Berger and Martin (2002), and Marin, Karageorghis and Lesnic (2009); Marin (2009a); Marin and Lesnic (2003), and Marin (2009b); and Marin (2006) who have solved a similar problem for the Laplace equation, FGMs, the Lamé system and Helmholtz-type equations, respectively. However, Zeb, Ingham and Lesnic (2008) successfully employed the zeroth-order Tikhonov regularization functional, without imposing any physical constraints on the  $x_2$ -coordinates of the unknown boundary  $\partial\Omega_2$ .

#### 4.2 Physical constraints

In order to retrieve an accurate and physically correct numerical solution of the inverse geometric problem investigated herein, the Tikhonov first-order functional given by Eq. (14) is minimized subject to the following simple bounds imposed on the components of the unknown vector  $\mathbf{z} = \left[ z_2^{(N_1+2)}, \dots, z_2^{(N_1+N_2)} \right]^T \in \mathbb{R}^{N_2-1}$ :

$$-\sqrt{R_S^2 - \left( z_1^{(i)} \right)^2} < z_2^{(i)} < \phi_1(z_2^{(i)}), \quad i = N_1 + 2, \dots, N_1 + N_2. \quad (18)$$

The simple bounds (18) require that the  $x_2$ -coordinates of the unknown boundary  $\partial\Omega_2$  be situated below those corresponding to the known boundary  $\partial\Omega_2$ , and the singularities be located outside  $\bar{\Omega}$ . Alternatively, one can impose different lower and/or upper bounds for the components of the unknown vector  $\mathbf{z}$ , provided that some additional *a priori* information about the location of the unknown boundary  $\partial\Omega_2$  is known. For example, if it is known that the  $x_2$ -coordinates of the unknown boundary  $\partial\Omega_2$  are situated below the  $x_1$ -axis, then the simple bounds (18) can be replaced by

$$-\sqrt{R_S^2 - \left( z_1^{(i)} \right)^2} < z_2^{(i)} < 0, \quad i = N_1 + 2, \dots, N_1 + N_2. \quad (19)$$

In summary, the Tikhonov regularization method solves a (physically) constrained minimization problem using a smoothness norm in order to provide a stable solution which both fits the data and possesses a minimum structure. More precisely, the MFS system of nonlinear equations (13a) – (13c) associated with the inverse geometric problem for two-dimensional Helmholtz-type equations given by Eqs. (2a) – (2d) is solved numerically by minimizing the Tikhonov first-order regularization functional (14) with respect to the unknown pair of vectors  $(\mathbf{c}, \mathbf{z}) \in \mathbb{R}^M \times \mathbb{R}^{N_2-1}$ , subject to the physical constraints (18) or (19), i.e.

$$(\mathbf{c}_\lambda, \mathbf{z}_\lambda) : \mathcal{F}_\lambda(\mathbf{c}_\lambda, \mathbf{z}_\lambda) = \min_{(\mathbf{c}, \mathbf{z}) \in \mathbb{R}^M \times \mathbb{R}^{N_2-1}} \left\{ \mathcal{F}_\lambda(\mathbf{c}, \mathbf{z}) \mid \mathbf{z} \text{ satisfies Eq. (18) or (19)} \right\}. \quad (20)$$

### 4.3 Numerical implementation

The minimization of the constrained Tikhonov first-order regularization functional (20) is obtained using the NAG subroutine E04UNF [NAG Library Mark 21 (2007)] which minimizes a sum of squares subject to constraints. This may include simple bounds, linear constraints and smooth nonlinear constraints. Each iteration of the subroutine E04UNF includes the following: (i) the solution of a quadratic programming subproblem; (ii) a line search with an augmented Lagrangian function; and (iii) a quasi-Newton update of the approximate Hessian of the Lagrangian function, see e.g. Gill, Murray and Wright (1981).

#### 4.3.1 Tikhonov regularization functional

In order to adjust our code to E04UNF, we denote by  $\boldsymbol{\eta} = (\mathbf{c}, \mathbf{z}) \in \mathbb{R}^{M+N_2-1}$ , i.e.

$$\boldsymbol{\eta}_\ell = \mathbf{c}_\ell, \quad \ell = 1, \dots, M; \quad \boldsymbol{\eta}_{M+\ell} = \mathbf{z}_2^{(M+\ell+1)}, \quad \ell = 1, \dots, N_2 - 1; \quad (21)$$

and we also recall that relation (8c) is satisfied. We then re-write the Tikhonov first-order regularization functional defined by Eq. (14) in the following form:

$$\begin{aligned} \mathcal{F}_\lambda(\cdot) : \mathbb{R}^{M+N_2-1} &\longrightarrow [0, \infty), \\ \mathcal{F}_\lambda(\boldsymbol{\eta}) &= \underbrace{\frac{1}{2} \sum_{i=1}^{2N_1+N_2} [\bar{y}_k - \bar{F}_k(\boldsymbol{\eta})]^2}_{= \mathcal{F}_{LS}(\mathbf{c}, \mathbf{z})} + \underbrace{\frac{1}{2} [\bar{y}_{2N_1+N_2+1} - \bar{F}_{2N_1+N_2+1}(\boldsymbol{\eta})]^2}_{= \mathcal{R}_\lambda(\mathbf{z})}, \end{aligned} \quad (22)$$

where the vectors  $\bar{\mathbf{F}}(\boldsymbol{\eta}) = [\bar{F}_1(\boldsymbol{\eta}), \dots, \bar{F}_{2N_1+N_2+1}(\boldsymbol{\eta})]^T \in \mathbb{R}^{2N_1+N_2+1}$  and  $\bar{\mathbf{y}} = [\bar{y}_1, \dots, \bar{y}_{2N_1+N_2+1}]^T \in \mathbb{R}^{2N_1+N_2+1}$  are given by

$$\bar{F}_k(\eta) = \sum_{j=1}^M G(\mathbf{x}^{(k)}, \xi^{(j)}) \mathbf{c}_j, \quad \bar{y}_k = \tilde{\mathbf{u}}(\mathbf{x}^{(k)}), \quad k = 1, \dots, N_1, \quad (23a)$$

$$\bar{F}_{N_1+k}(\eta) = \sum_{j=1}^M H(\mathbf{x}^{(k)}, \xi^{(j)}) \mathbf{c}_j, \quad \bar{y}_{N_1+k} = \tilde{\mathbf{q}}(\mathbf{x}^{(k)}), \quad k = 1, \dots, N_1, \quad (23b)$$

$$\bar{F}_{2N_1+k}(\eta) = \sum_{j=1}^M \left[ \alpha_u G(\mathbf{x}^{(N_1+k)}, \xi^{(j)}) + \alpha_q H(\mathbf{x}^{(N_1+k)}, \xi^{(j)}) \right] \mathbf{c}_j, \quad (23c)$$

$$\bar{y}_{2N_1+k} = \tilde{\mathbf{f}}(\mathbf{x}^{(N_1+k)}), \quad k = 1, \dots, N_2,$$

$$\bar{F}_{2N_1+N_2+1}(\eta) = \sqrt{2\lambda} \left[ \sum_{j=2}^{N_2+1} \left( z_2^{(N_1+j)} - z_2^{(N_1+j-1)} \right)^2 \right]^{1/2}, \quad \bar{y}_{2N_1+N_2+1} = 0. \quad (23d)$$

#### 4.3.2 Gradient of the Tikhonov regularization functional

We define the components of the gradient,  $\mathbf{J}(\eta) = \nabla \mathcal{F}_\lambda(\eta) \in \mathbb{R}^{(2N_1+N_2+1) \times (M+N_2-1)}$ , corresponding to the Tikhonov first-order regularization functional, as defined in Eq. (22), by

$$\mathbf{J}_{k,\ell}(\eta) = \begin{cases} G(\mathbf{x}^{(k)}, \xi^{(\ell)}), & k = 1, \dots, N_1, \quad \ell = 1, \dots, M, \\ 0, & k = 1, \dots, N_1, \quad \ell = M+1, \dots, M+N_2-1, \end{cases} \quad (24a)$$

$$\mathbf{J}_{N_1+k,\ell}(\eta) = \begin{cases} H(\mathbf{x}^{(k)}, \xi^{(\ell)}), & k = 1, \dots, N_1, \quad \ell = 1, \dots, M, \\ 0, & k = 1, \dots, N_1, \quad \ell = M+1, \dots, M+N_2-1, \end{cases} \quad (24b)$$

$$\mathbf{J}_{2N_1+k,\ell}(\eta) = \begin{cases} \alpha_u G(\mathbf{x}^{(N_1+k)}, \xi^{(\ell)}) + \alpha_q H(\mathbf{x}^{(N_1+k)}, \xi^{(\ell)}), & k = 1, \dots, N_2, \quad \ell = 1, \dots, M, \\ \sum_{j=1}^M \frac{\partial}{\partial \eta_\ell} \left[ \alpha_u G(\mathbf{x}^{(N_1+k)}, \xi^{(j)}) + \alpha_q H(\mathbf{x}^{(N_1+k)}, \xi^{(j)}) \right] \mathbf{c}_j, & k = 1, \dots, N_2, \quad \ell = M+1, \dots, M+N_2-1, \end{cases} \quad (24c)$$

$$\mathbf{J}_{2N_1+N_2+1,\ell}(\eta) = \begin{cases} 0, & \ell = 1, \dots, M, \\ \sqrt{2\lambda} \frac{\partial}{\partial \eta_\ell} \|\mathbf{z}'\|, & \ell = M+1, \dots, M+N_2-1. \end{cases} \quad (24d)$$

It should be mentioned that providing as many exact values for the components of the gradient  $\mathbf{J}(\eta) = \nabla \mathcal{F}_\lambda(\eta)$  as possible to the NAG subroutine E04UNF results not only in an improvement in the accuracy of the numerical approximation of the unknown boundary, but also in a marked decrease in the computational time required to minimize the Tikhonov first-order regularization functional given by (14) with respect to the unknown vector  $\eta \in \mathbb{R}^{M+N_2-1}$ , subject to the physical constraints (18) or (19).

### 5 Numerical results and discussion

In this section we investigate the performance of the proposed numerical method, namely the regularized MFS described in Section 4. To do so, we solve numerically the inverse geometric problem given by Eqs. (2a) – (2d) for the two-dimensional modified Helmholtz equation, i.e.  $\mathcal{L} \equiv \Delta - \kappa^2$ , in the two-dimensional geometries which are schematically presented in Figs. 2(a)–(d). It should be mentioned that similar numerical results have been obtained for the inverse problem (2a) – (2d) associated with the two-dimensional Helmholtz equation, i.e.  $\mathcal{L} \equiv \Delta + \kappa^2$ , and therefore only one such example is included in this section (Example 5), for completeness.

#### 5.1 Examples

In Examples 1 – 4, we consider the following analytical solution for the temperature

$$u^{(an)}(\mathbf{x}) = e^{a_1 x_1 + a_2 x_2}, \quad \mathbf{x} = (x_1, x_2) \in \overline{\Omega}, \tag{25}$$

where  $\kappa = 2.0$ ,  $a_1 = 1.0$  and  $a_2 = -\sqrt{\kappa^2 - a_1^2} = -\sqrt{3}$ , whilst the corresponding analytical normal heat flux on the boundary  $\partial\Omega$  is given by

$$q^{(an)}(\mathbf{x}) = [a_1 n_1(\mathbf{x}) + a_2 n_2(\mathbf{x})] e^{a_1 x_1 + a_2 x_2}, \quad \mathbf{x} = (x_1, x_2) \in \partial\Omega. \tag{26}$$

**Example 1.** We consider the unit disk  $\Omega = \{\mathbf{x} = (x_1, x_2) \mid x_1^2 + x_2^2 < r^2\}$ ,  $r = 1.0$ , whose boundary  $\partial\Omega$  consists of two parts, namely

$$\partial\Omega_1 = \left\{ \mathbf{x} = (x_1, x_2) \mid -1 \leq x_1 \leq 1; x_2 = \sqrt{r^2 - x_1^2} \right\} \tag{27a}$$

and

$$\partial\Omega_2 = \left\{ \mathbf{x} = (x_1, x_2) \mid -1 < x_1 < 1; x_2 = -\sqrt{r^2 - x_1^2} \right\}. \tag{27b}$$

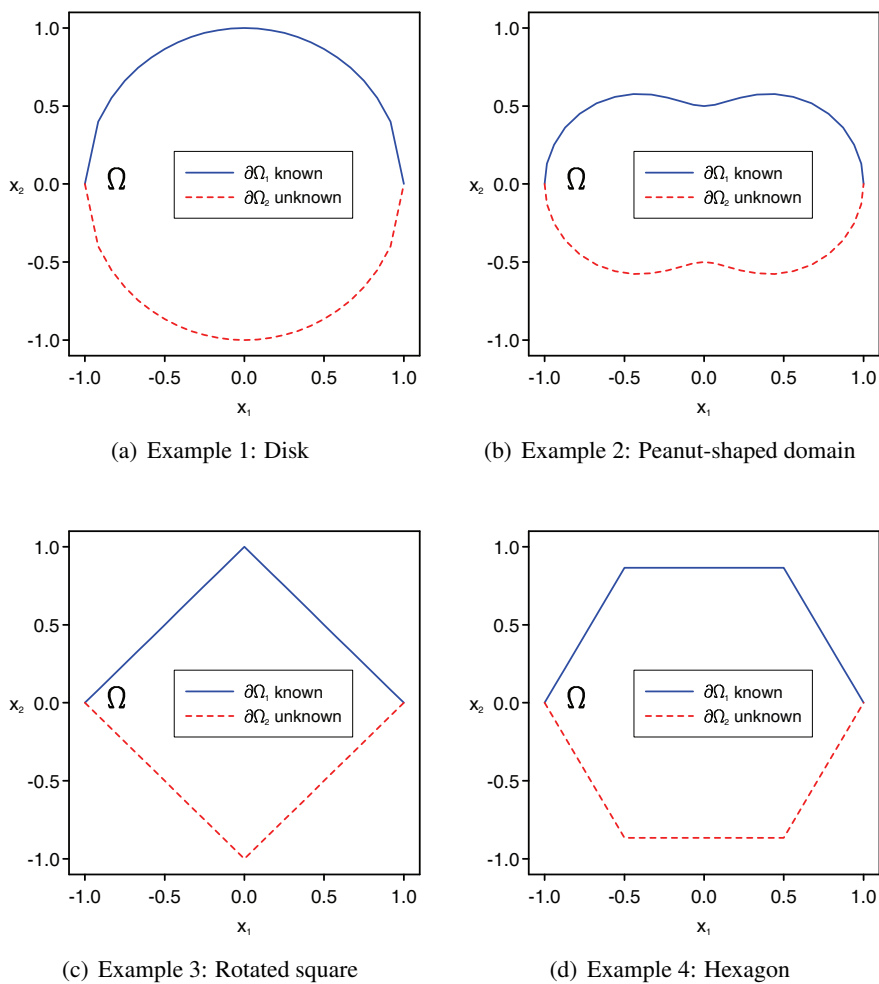


Figure 2: Schematic diagram of the domain  $\Omega$ , and the known and unknown boundaries  $\partial\Omega_1$  and  $\partial\Omega_2$ , respectively, for the inverse geometric problems analysed.

**Example 2.** We consider the peanut-shaped domain  $\Omega = \{ \mathbf{x} = (x_1, x_2) \mid x_1^2 + x_2^2 < r^2(\theta); \theta \in [0, 2\pi) \}$ , where  $r^2(\theta) = \cos^2(\theta) + \frac{1}{4} \sin^2(\theta)$ , which is bounded by the following curves

$$\partial\Omega_1 = \{ \mathbf{x} = (x_1, x_2) \mid x_1 = r(\theta) \cos(\theta); x_2 = r(\theta) \sin(\theta); \theta \in [0, \pi] \} \tag{28a}$$

and

$$\partial\Omega_2 = \{ \mathbf{x} = (x_1, x_2) \mid x_1 = r(\theta) \cos(\theta); x_2 = r(\theta) \sin(\theta); \theta \in (\pi, 2\pi) \}. \tag{28b}$$

**Example 3.** We consider the domain  $\Omega$  as the square  $(-r/\sqrt{2}, r/\sqrt{2})^2$ ,  $r = 1.0$ , rotated by an angle  $\theta = \pi/4$ , whose boundary  $\partial\Omega$  consists of two parts, namely

$$\begin{aligned} \partial\Omega_1 &= \{ \mathbf{x} = (x_1, x_2) \mid 0 \leq x_1 \leq r; x_2 = r - x_1 \} \\ &\cup \{ \mathbf{x} = (x_1, x_2) \mid -r \leq x_1 \leq 0; x_2 = r + x_1 \} \end{aligned} \tag{29a}$$

and

$$\begin{aligned} \partial\Omega_2 &= \{ \mathbf{x} = (x_1, x_2) \mid -r < x_1 \leq 0; x_2 = -(r + x_1) \} \\ &\cup \{ \mathbf{x} = (x_1, x_2) \mid 0 \leq x_1 < r; x_2 = -(r - x_1) \}. \end{aligned} \tag{29b}$$

**Example 4.** We consider the regular hexagonal domain  $\Omega$  inscribed in the circle  $\partial B(0; r) = \{ \mathbf{x} = (x_1, x_2) \mid x_1^2 + x_2^2 = r^2 \}$ ,  $r = 1.0$ , which is bounded by the following curves

$$\begin{aligned} \partial\Omega_1 &= \left\{ \mathbf{x} = (x_1, x_2) \mid \frac{r}{2} < x_1 \leq r; x_2 = (r - x_1) \sqrt{3} \right\} \\ &\cup \left\{ \mathbf{x} = (x_1, x_2) \mid -\frac{r}{2} \leq x_1 \leq \frac{r}{2}; x_2 = r \frac{\sqrt{3}}{2} \right\} \\ &\cup \left\{ \mathbf{x} = (x_1, x_2) \mid -r \leq x_1 < -\frac{r}{2}; x_2 = (r + x_1) \sqrt{3} \right\} \end{aligned} \tag{30a}$$

and

$$\begin{aligned} \partial\Omega_2 &= \left\{ \mathbf{x} = (x_1, x_2) \mid -r < x_1 < -\frac{r}{2}; x_2 = -(r + x_1) \sqrt{3} \right\} \\ &\cup \left\{ \mathbf{x} = (x_1, x_2) \mid -\frac{r}{2} \leq x_1 \leq \frac{r}{2}; x_2 = -r \frac{\sqrt{3}}{2} \right\} \\ &\cup \left\{ \mathbf{x} = (x_1, x_2) \mid \frac{r}{2} < x_1 < r; x_2 = -(r - x_1) \sqrt{3} \right\}. \end{aligned} \tag{30b}$$

The inverse geometric problems investigated in this paper have been solved using a uniform distribution of both the MFS boundary collocation points  $\mathbf{x}^{(i)}$ ,  $i = 1, \dots, N$ , and the singularities  $\xi^{(j)}$ ,  $j = 1, \dots, M$ , as described in Sections 3.1 and 3.3, respectively, with  $N_1 = N_2 = 12$ ,  $M = N = N_1 + N_2$  and  $R_S = 2.0$ . Also, the Tikhonov first-order regularization functional (14) has been minimized subject to the physical constraints (19), see also Eq. (20), and this is consistent with the shape of the unknown boundary  $\partial\Omega_2$  considered in Examples 1–4, see Eqs. (27b), (28b), (29b) and (30b). Moreover, in all examples, the initial guesses for the unknown MFS coefficients  $\mathbf{c} = [c_1, \dots, c_M]^T$  and the unknown  $x_2$ -coordinates  $\mathbf{z} = [z_2^{(N_1+2)}, \dots, z_2^{(N_1+N_2)}]^T$  of the boundary points that determine the unknown boundary  $\partial\Omega_2$  were taken as:

- (i)  $\eta_\ell = c_\ell = 1.0 \times 10^0$ ,  $\ell = 1, \dots, M$ ;
- (ii)  $\eta_{M+\ell} = z_2^{(M+\ell+1)} = -1.0 \times 10^{-15}$ ,  $\ell = 1, \dots, N_2 - 1$ .

## 5.2 Numerical results obtained without regularization

In what follows, the temperature,  $u|_{\partial\Omega_1} = u^{(\text{an})}|_{\partial\Omega_1}$ , and/or the normal heat flux,  $q|_{\partial\Omega_1} = q^{(\text{an})}|_{\partial\Omega_1}$ , on the known boundary have been perturbed as

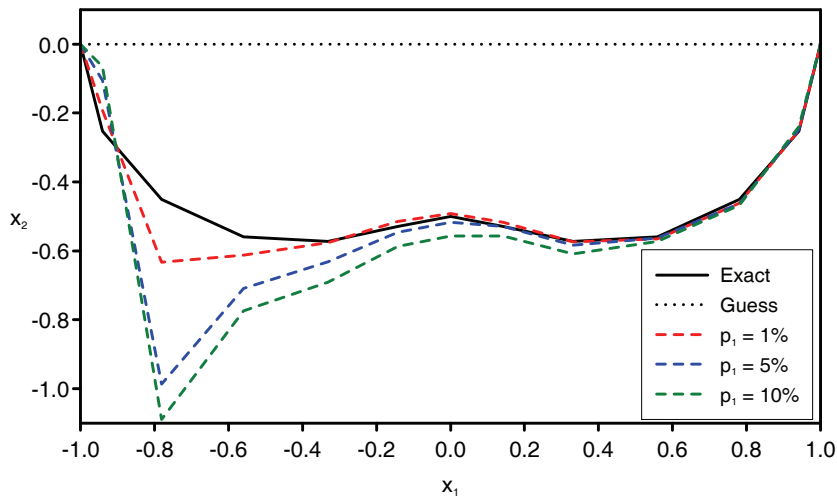
$$\tilde{u}^\varepsilon|_{\partial\Omega_1} = u|_{\partial\Omega_1} + \delta u, \quad \delta u = \text{G05DDF}(0, \sigma_1), \quad \sigma_1 = \max_{\partial\Omega_1} |u| \times (p_1/100), \quad (31)$$

and

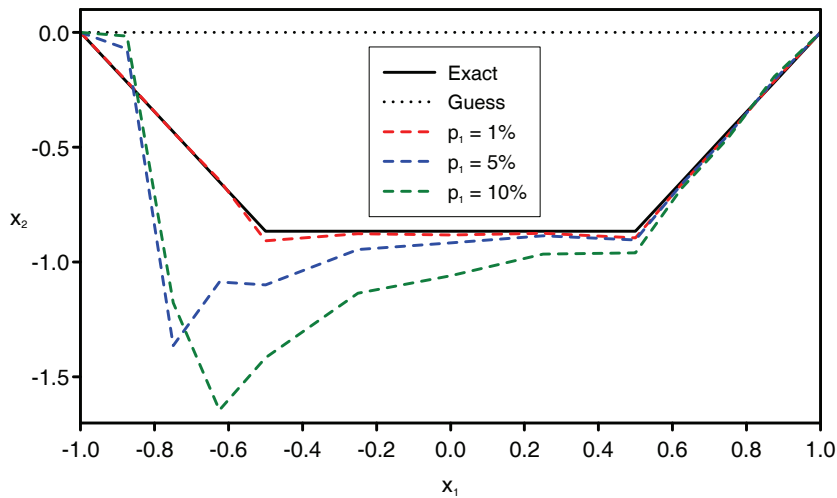
$$\tilde{q}^\varepsilon|_{\partial\Omega_1} = q|_{\partial\Omega_1} + \delta q, \quad \delta q = \text{G05DDF}(0, \sigma_2), \quad \sigma_2 = \max_{\partial\Omega_1} |q| \times (p_2/100), \quad (32)$$

respectively. Here  $\delta u$  and  $\delta q$  are Gaussian random variables with mean zero and standard deviations  $\sigma_1$  and  $\sigma_2$ , respectively, generated by the NAG subroutine G05DDF [NAG Library Mark 21 (2007)], while  $p_1\%$  and  $p_2\%$  are the percentages of the added noise included in the input boundary temperature,  $u|_{\partial\Omega_1}$ , and normal heat flux,  $q|_{\partial\Omega_1}$ , respectively, in order to simulate the inherent measurement errors.

The initial guess and the exact and reconstructed shapes of the boundary  $\partial\Omega_2$ , obtained using the least-squares method functional (15) subject to the physical constraints (19), perturbed Dirichlet data on  $\partial\Omega_1$ ,  $\alpha_u = 1$  and  $\alpha_q = 0$ , in the case of Examples 2 and 4 are illustrated in Figs. 3(a) and 3(b), respectively. As can be observed from these figures, the MFS approximations are poor and oscillatory and, in some cases unbounded, i.e. unstable. Hence, Figs. 3(a) and 3(b) indicate the necessity of employing regularization methods to obtain accurate and stable solutions



(a) Example 2



(b) Example 4

Figure 3: Initial guess, exact and reconstructed shapes of the boundary  $\partial\Omega_2$ , obtained using the least-squares method, perturbed Dirichlet data on  $\partial\Omega_1$ ,  $\alpha_u = 1$  and  $\alpha_q = 0$ , for (a) Example 2, and (b) Example 4.

to the problems investigated. Similar results have been obtained for the other examples considered in this paper, as well as for exact Neumann or Robin conditions prescribed on the unknown boundary,  $\partial\Omega_2$ , which are therefore not presented.

### 5.3 Accuracy errors

In order to analyse the accuracy of the numerical results obtained for the unknown boundary,  $\partial\Omega_2$ , of the two-dimensional domain,  $\Omega$ , occupied by an FGM, using various values of the regularization parameter,  $\lambda > 0$ , we define the *root mean-square (RMS) error* by

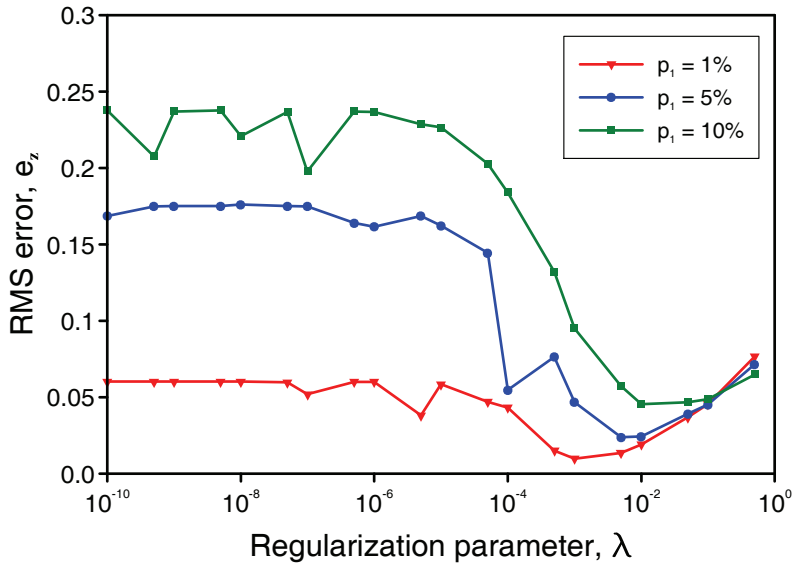
$$e_z(\lambda) = \sqrt{\frac{1}{N_2 - 1} \sum_{i=N_1+2}^{N_1+N_2} \left( z_2^{(i;\lambda)} - z_2^{(i;\text{an})} \right)^2}, \quad \lambda > 0, \quad (33)$$

where  $z_2^{(i;\lambda)}$  is the numerically retrieved value corresponding to the regularization parameter,  $\lambda > 0$ , for the exact  $x_2$ -coordinate,  $z_2^{(i;\text{an})}$  that determines the unknown boundary,  $\partial\Omega_2$ .

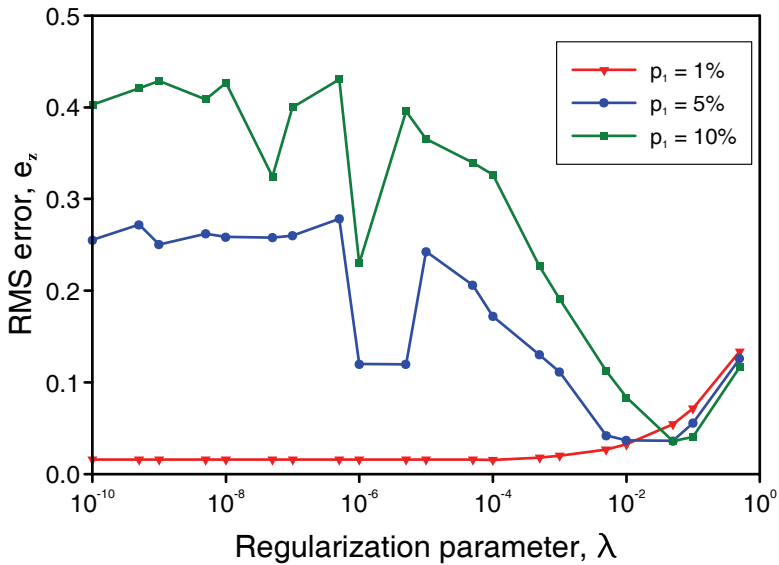
Figs. 4(a) and 4(b) present on a log-log scale the RMS error,  $e_z$ , defined by Eq. (33), as a function of the regularization parameter,  $\lambda$ , obtained using the MFS-based Tikhonov first-order regularization method described in Section 4, various levels of noise added into the boundary temperature data  $u|_{\partial\Omega_1}$ , namely  $p_1 \in \{1\%, 5\%, 10\%\}$ ,  $\alpha_u = 1$  and  $\alpha_q = 0$ , for the inverse geometric problems given by Examples 2 and 4, respectively. From these figures it can be seen that, for each level of noise, the RMS error  $e_z$  reaches its minimum for an optimal value of the regularization parameter,  $\lambda = \lambda_{\text{opt}}$ . Moreover, the minimum in the error  $e_z$  decreases as the level of noise added into the Dirichlet data on  $\partial\Omega_1$  increases.

### 5.4 Selection of the optimal regularization parameter

The performance of regularization methods depends a lot on a suitable choice of the regularization parameter. One extensively studied criterion is the discrepancy principle, see e.g. Morozov (1966). Although this criterion is mathematically rigorous, it requires a reliable estimation of the amount of noise added to the data which may not be available for practical problems. Heuristic approaches are preferable in the case when no *a priori* information about the noise is available. Several heuristic approaches have been proposed for the Tikhonov regularization method, including the L-curve criterion, see Hansen (1998), and the generalized cross-validation, see Wahba (1977). In this study, we employ the L-curve criterion to determine the optimal regularization parameter,  $\lambda_{\text{opt}}$ .

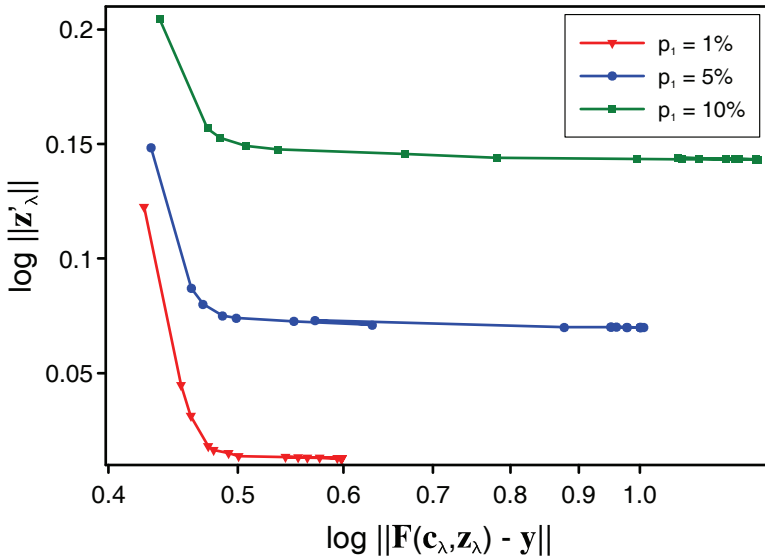


(a) Example 2

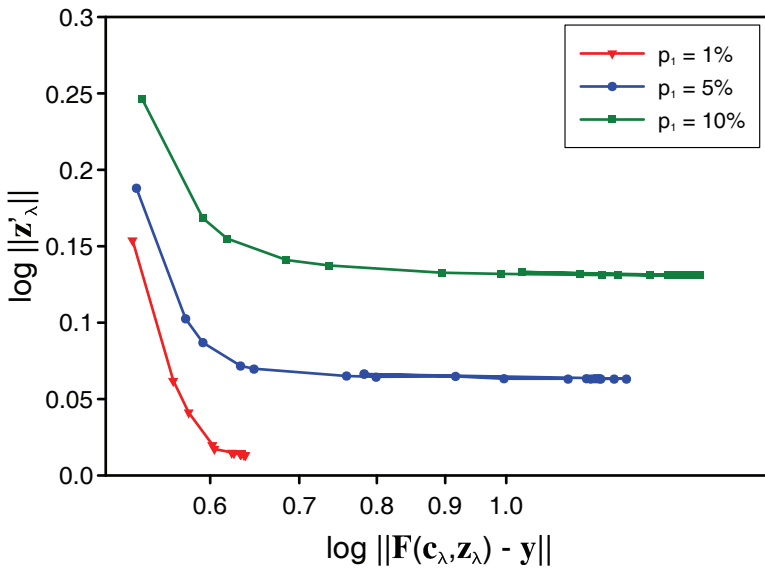


(b) Example 4

Figure 4: The RMS error,  $e_z$ , as a function of the regularization parameter,  $\lambda$ , obtained using the Tikhonov regularization method, perturbed Dirichlet data on  $\partial\Omega_1$ ,  $\alpha_u = 1$  and  $\alpha_q = 0$ , for (a) Example 2, and (b) Example 4.



(a) Example 2



(b) Example 4

Figure 5: The L-curves obtained using the Tikhonov regularization method, perturbed Dirichlet data on  $\partial\Omega_1$ ,  $\alpha_u = 1$  and  $\alpha_q = 0$ , for (a) Example 2, and (b) Example 4.

If we define on a logarithmic scale the following curve

$$\left\{ \left( \sqrt{2\mathcal{F}_{LS}(\eta_\lambda)}, \sqrt{2\mathcal{R}(\mathbf{z}_\lambda)} \right) \mid \lambda > 0 \right\} = \left\{ \left( \|\mathbf{F}(\eta_\lambda) - \mathbf{y}\|, \|\mathbf{z}'_\lambda\| \right) \mid \lambda > 0 \right\}, \quad (34)$$

where  $\mathbf{F}(\eta) = [\bar{\mathbf{F}}_1(\eta), \dots, \bar{\mathbf{F}}_{N_1+N_2}(\eta)]^\top$  and  $\mathbf{y} = [\bar{y}_1, \dots, \bar{y}_{N_1+N_2}]^\top$ , then typically this has an L-shaped form and hence it is referred to as the L-curve. According to the L-curve criterion, the optimal regularization parameter corresponds to the corner of the L-curve since a good tradeoff between the residual and solution norms is achieved at this point. Numerically, the L-curve method is robust and stable with respect to both uncorrelated and highly correlated noise. Furthermore, this criterion works effectively for certain classes of practical problems, see Hansen (1998) and Chen, Chen, Hong and Chen (1995). For a discussion of the theoretical aspects of the L-curve criterion, we refer the reader to Hanke (1996) and Vogel (1996).

Figs. 5(a) and 5(b) clearly illustrate the L-shaped curves retrieved using the Tikhonov regularization method and perturbed temperature data on the known boundary,  $\partial\Omega_1$  ( $\alpha_u = 1$  and  $\alpha_q = 0$ ), in the case of Examples 2 and 4, respectively. The corresponding values for the optimal regularization parameter,  $\lambda_{\text{opt}}$ , obtained according to this criterion, are as follows:

- (i)  $\lambda_{\text{opt}} = 1.0 \times 10^{-3}$ ,  $\lambda_{\text{opt}} = 5.0 \times 10^{-3}$  and  $\lambda_{\text{opt}} = 1.0 \times 10^{-2}$  for  $p_1 = 1\%$ ,  $p_1 = 5\%$ , and  $p_1 = 10\%$ , respectively, in the case of Example 2;
- (ii)  $\lambda_{\text{opt}} = 1.0 \times 10^{-4}$  and  $\lambda_{\text{opt}} = 5.0 \times 10^{-2}$  for  $p_1 = 1\%$  and  $p_1 = 5\%, 10\%$ , respectively, in the case of Example 4.

Comparing Figs. 4 and 5, it can be observed that, for both Examples 2 and 4 and all levels of noise added into the Dirichlet data on  $\partial\Omega_1$ , the minimum in the RMS error,  $e_z$ , is attained for  $\lambda \approx \lambda_{\text{opt}}$ , with  $\lambda_{\text{opt}}$  given by the L-curve criterion. Similar results have been obtained for the other inverse geometric problems investigated and hence they are not presented. We can therefore conclude that Hansen's L-curve criterion provides a very good approximation for the optimal regularization parameters.

### 5.5 Numerical results obtained with regularization

Figs. 6(a) and 6(b) show the initial guess, the exact and numerical shapes of the unknown boundary,  $\partial\Omega_2$ , obtained for the inverse geometric problem (2a) – (2d) with  $\alpha_u = 0$  and  $\alpha_q = 1$ , using the regularized MFS algorithm described in Section 4, the optimal regularization parameter,  $\lambda = \lambda_{\text{opt}}$ , chosen according to the L-curve criterion, and various levels of noise added into the temperature  $u|_{\partial\Omega_1}$  and the normal heat flux  $q|_{\partial\Omega_1}$ , respectively, in the case of Example 1. From these figures, it can be observed that the numerical solutions are stable and consistent with respect

to the amounts of noise  $p_1$  and  $p_2$  added to the input Dirichlet and Neumann data, respectively, on the accessible boundary  $\partial\Omega_1$ . Moreover, in both cases considered, the numerically retrieved solutions converge to the exact solution (27b).

The MFS-based Tikhonov first-order regularization method presented in Section 4, in conjunction with Hansen's L-curve criterion for determining the optimal value of the regularization parameter, produces stable and consistent numerical solutions with respect to the amount of noise added to the Cauchy data on the known part of the boundary,  $\partial\Omega_1$ . These solutions are both accurate approximations and converge to the exact solution, also in the case of two-dimensional non-convex domains with a smooth boundary, such as the peanut-shaped domain considered in Example 2, see Eq. (28). These results can be observed in Figs. 7(a) and 7(b) which illustrate the initial guess, the exact and numerically retrieved shapes of the unknown boundary given by Eq. (28b), obtained with a perturbed temperature  $u|_{\partial\Omega_1}$ , i.e.  $p_1 = 1\%, 5\%$  and  $10\%$ , with given Dirichlet and Neumann data on  $\partial\Omega_2$ , respectively.

The proposed MFS-Tikhonov regularization procedure works equally well for domains bounded by a piecewise smooth boundary, such as the rotated square and the hexagonal domain considered in Examples 3 and 4, respectively. The initial guess and the exact and numerical shapes of the unknown boundary,  $\partial\Omega_2$ , in the case of Examples 3 and 4, obtained using the regularization method presented in Section 4, the optimal regularization parameter,  $\lambda = \lambda_{\text{opt}}$ , selected by Hansen's L-curve criterion, and various levels of noise added into the Cauchy data, are shown in Figs. 8 and 9, respectively. In both Examples 3 and 4, we observe that the corners are, as expected, slightly rounded-off since the minimization of the Tikhonov first-order regularization functional (14) subject to the physical constraints (19) forces the numerical solution to be smooth.

**Example 5.** We finally consider the geometry of Example 1 and the corresponding inverse problem governed by the Helmholtz equation with the analytical solutions for the temperature and normal heat flux on  $\partial\Omega$  are given by

$$\mathbf{u}^{(\text{an})}(\mathbf{x}) = \cos(a_1 x_1 + a_2 x_2), \quad \mathbf{x} = (x_1, x_2) \in \overline{\Omega}, \quad (35a)$$

and

$$\mathbf{q}^{(\text{an})}(\mathbf{x}) = -[a_1 n_1(\mathbf{x}) + a_2 n_2(\mathbf{x})] \sin(a_1 x_1 + a_2 x_2), \quad \mathbf{x} = (x_1, x_2) \in \partial\Omega, \quad (35b)$$

respectively, where  $\kappa = 1.0$  and  $a_1 = a_2 = \sqrt{2}/2$ . In Fig. 10 we present the results corresponding to Fig. 6. As can be observed from this figure, the behaviour of the numerical solution for this problem is very similar to that of the problem governed by the modified Helmholtz equation.

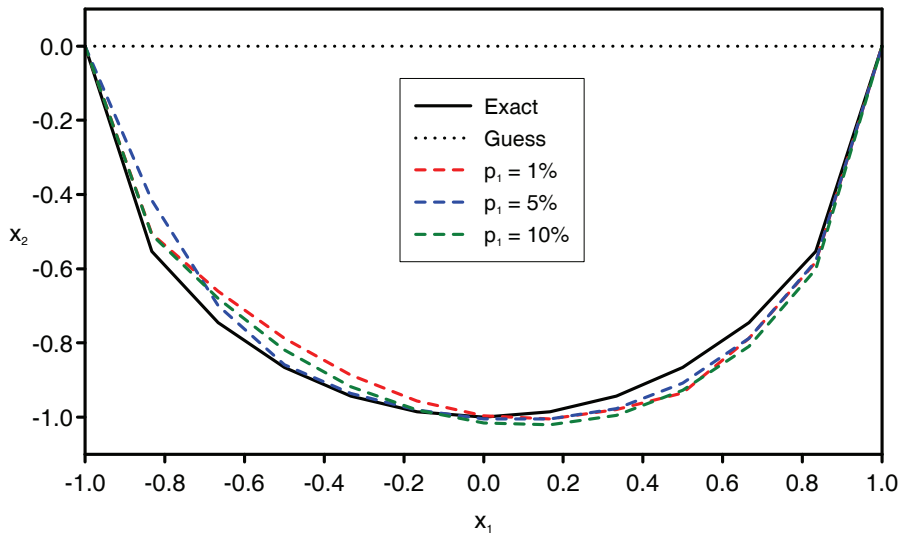
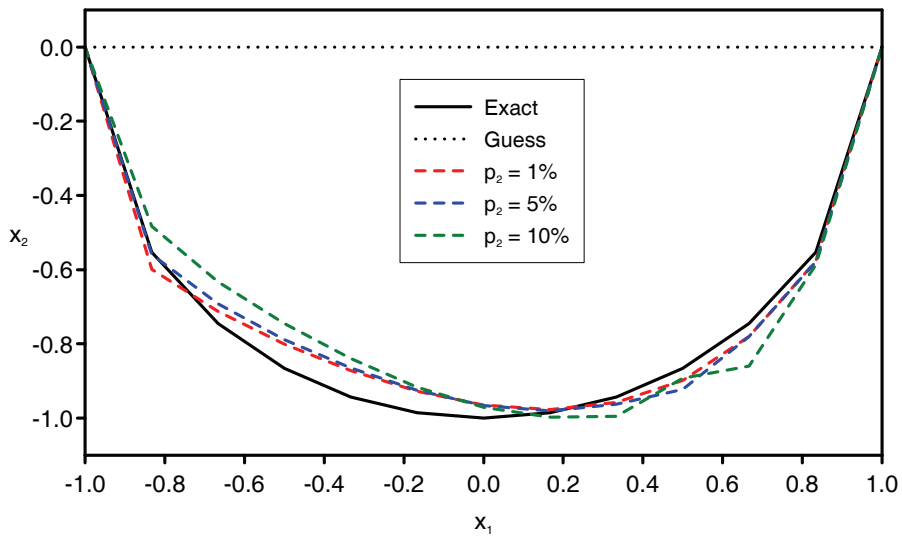
(a) Perturbed Dirichlet data on  $\partial\Omega_1$ (b) Perturbed Neumann data on  $\partial\Omega_1$ 

Figure 6: Initial guess, exact and reconstructed shapes of the boundary  $\partial\Omega_2$ , obtained using the Tikhonov regularization method,  $\alpha_u = 0$  and  $\alpha_q = 1$ , and perturbed (a) Dirichlet, and (b) Neumann data on  $\partial\Omega_1$ , in the case of Example 1.

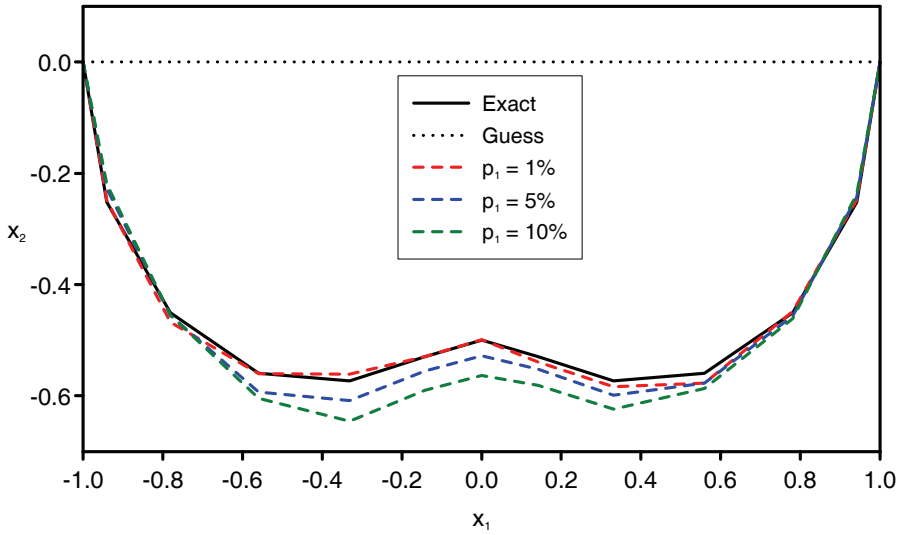
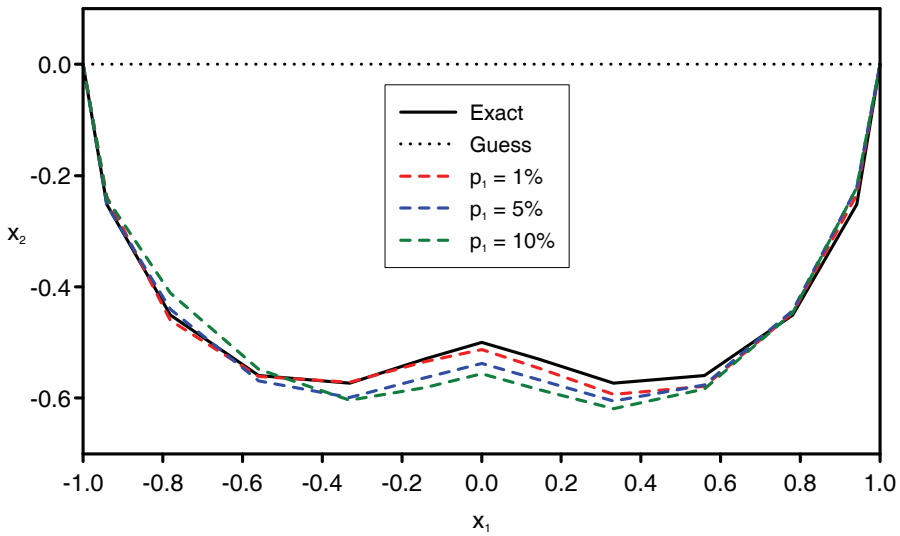
(a)  $\alpha_u = 1$  and  $\alpha_q = 0$ (b)  $\alpha_u = 0$  and  $\alpha_q = 1$ 

Figure 7: Initial guess, exact and reconstructed shapes of the boundary  $\partial\Omega_2$ , obtained using the Tikhonov regularization method, perturbed Dirichlet data on  $\partial\Omega_1$ , (a)  $\alpha_u = 1$  and  $\alpha_q = 0$ , and (b)  $\alpha_u = 0$  and  $\alpha_q = 1$ , in the case of Example 2.

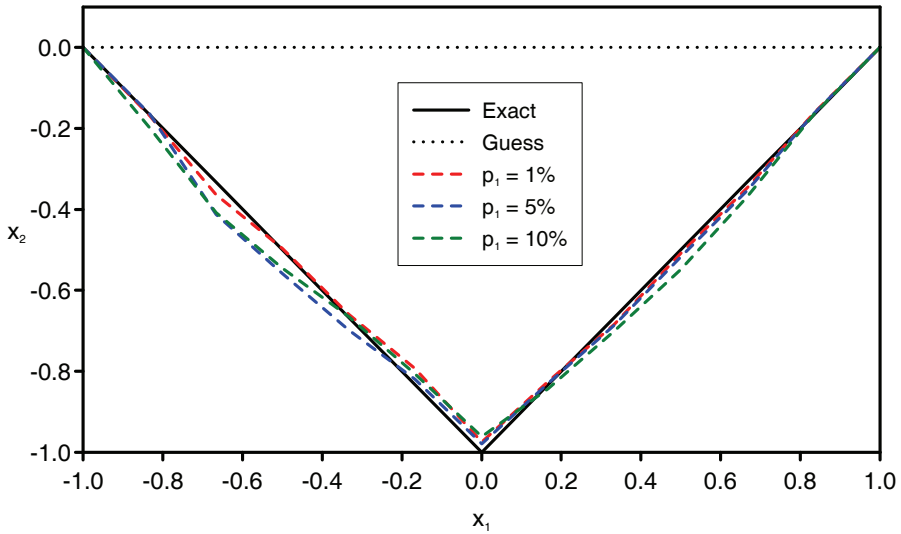
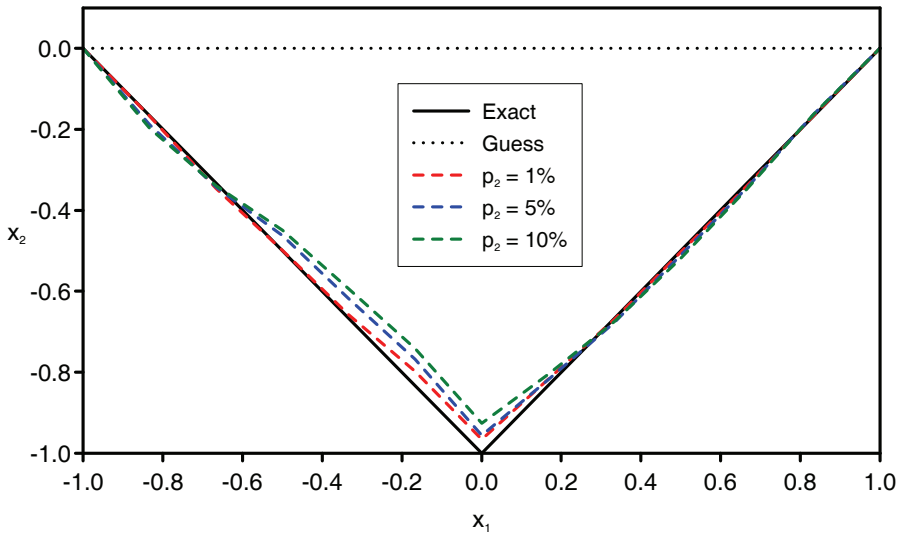
(a) Perturbed Dirichlet data on  $\partial\Omega_1$ (b) Perturbed Neumann data on  $\partial\Omega_1$ 

Figure 8: Initial guess, exact and reconstructed shapes of the boundary  $\partial\Omega_2$ , obtained using the Tikhonov regularization method,  $\alpha_u = 1$  and  $\alpha_q = 0$ , and perturbed (a) Dirichlet, and (b) Neumann data on  $\partial\Omega_1$ , in the case of Example 3.

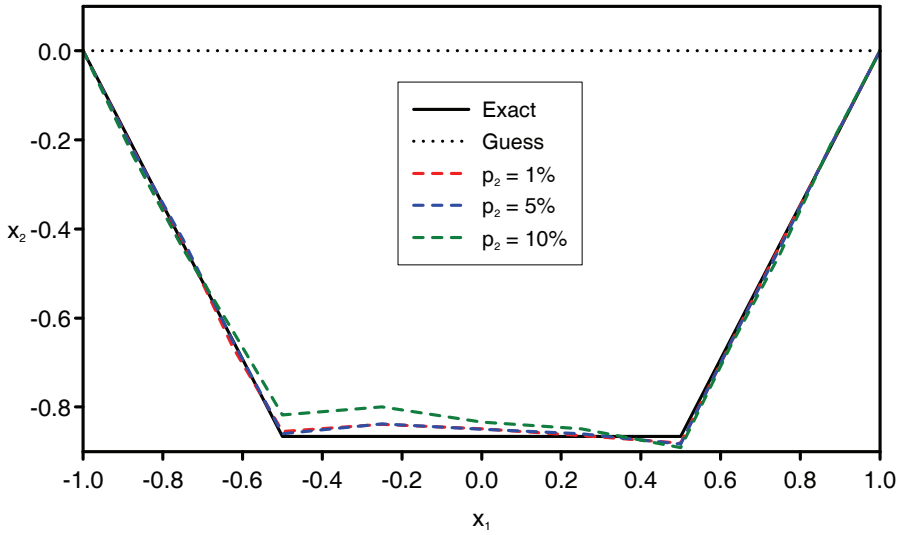
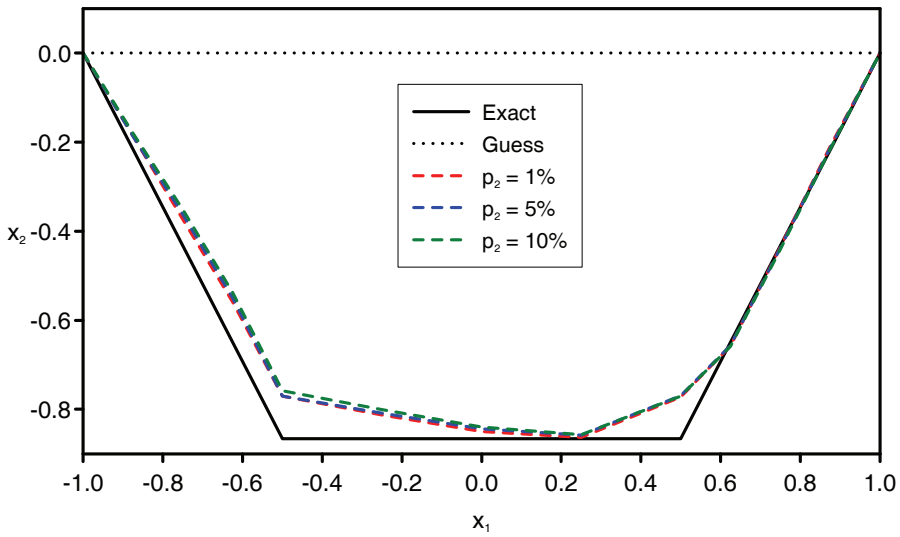
(a)  $\alpha_u = 1$  and  $\alpha_q = 0$ (b)  $\alpha_u = 0$  and  $\alpha_q = 1$ 

Figure 9: Initial guess, exact and reconstructed shapes of the boundary  $\partial\Omega_2$ , obtained using the Tikhonov regularization method, perturbed Neumann data on  $\partial\Omega_1$ , (a)  $\alpha_u = 1$  and  $\alpha_q = 0$ , and (b)  $\alpha_u = 0$  and  $\alpha_q = 1$ , in the case of Example 4.

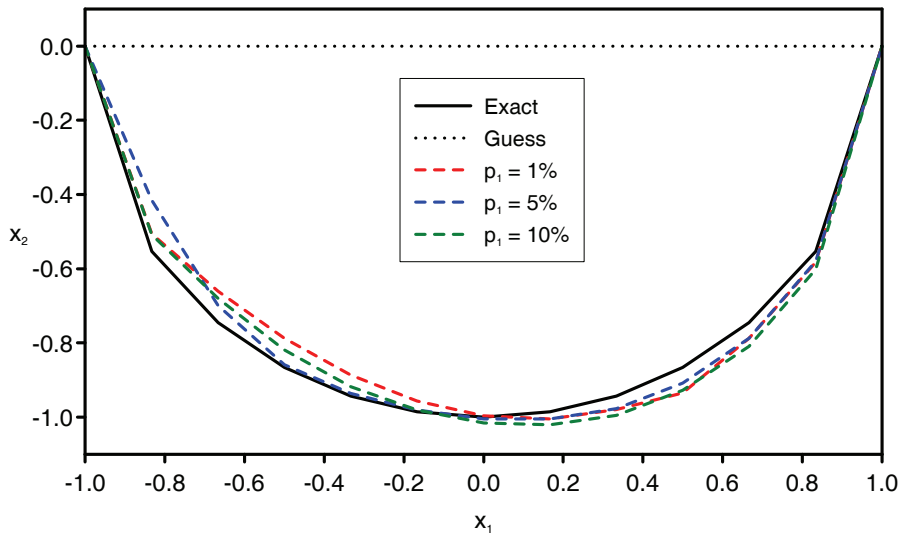
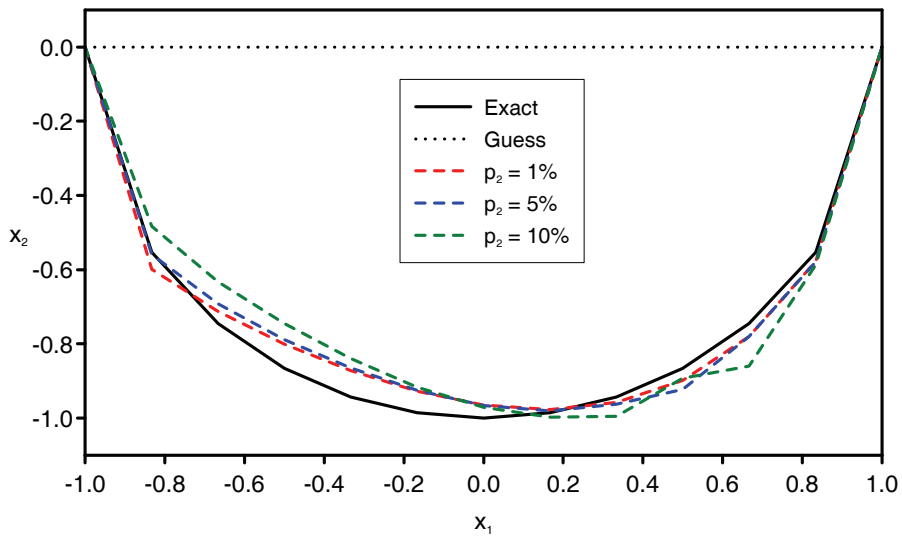
(a) Perturbed Dirichlet data on  $\partial\Omega_1$ (b) Perturbed Neumann data on  $\partial\Omega_1$ 

Figure 10: Initial guess, exact and reconstructed shapes of the boundary  $\partial\Omega_2$ , obtained using the Tikhonov regularization method,  $\alpha_u = 0$  and  $\alpha_q = 1$ , and perturbed (a) Dirichlet, and (b) Neumann data on  $\partial\Omega_1$ , in the case of Example 5.

Although not included in this paper, convergent, consistent and stable numerical approximations for the inaccessible boundary,  $\partial\Omega_2$ , have also been obtained for noisy Cauchy data on the accessible part of the boundary,  $\partial\Omega_1$ , and an exact Robin condition ( $\alpha_u \alpha_q \neq 0$ ) on the inaccessible and unknown boundary,  $\partial\Omega_2$ .

## 6 Conclusions

In this paper, the MFS was successfully applied for obtaining stable and accurate solutions of inverse problems associated with two-dimensional Helmholtz-type equations, namely the detection of an unknown portion of the boundary from a given exact boundary condition on this part of the boundary and additional noisy Cauchy data on the remaining known portion of the boundary. This inverse geometric problem is ill-posed and in discrete form yields an ill-conditioned system of nonlinear equations, which was solved in a stable manner by using the Tikhonov first-order regularization method. The optimal value of the regularization parameter was chosen according to Hansen's L-curve criterion. Several examples for two-dimensional simply connected, convex and non-convex domains, in which the (modified) Helmholtz equation is satisfied and having smooth and piecewise smooth boundaries, were considered. From the numerical experiments, it can be concluded that the proposed method is consistent and stable with respect to decreasing the amount of noise added to the Cauchy data. Furthermore, it is accurate and computationally very efficient. Moreover, since Helmholtz-type operators and their associated boundary conditions are linear, it can be concluded that the same observations as the ones obtained for the cases examined also hold in the case where the additional boundary measurements available on the accessible boundary are given by Robin-type conditions.

**Acknowledgement:** The authors would like to acknowledge the financial support received from the University of Cyprus.

## References

- Alves, C. J. S.; Antunes, P. R. S.** (2005): The method of fundamental solutions applied to the calculation of eigenfrequencies and eigenmodes of 2D simply connected shapes. *CMC: Computers, Materials & Continua*, vol. 2, pp. 251–265.
- Aparicio, N. D.; Pidcock, M. K.** (1996): The boundary inverse problem for the Laplace equation in two dimensions. *Inverse Problems*, vol. 12, pp. 565–577.
- Beretta, E.; Vessela, S.** (1998): Stable determination of boundaries from Cauchy data. *SIAM Journal of Mathematical Analysis*, vol. 30, pp. 220–232.

**Bukhgeim, A. L.; Cheng, J.; Yamamoto, M.** (1999): Stability for an inverse problem of determining a part of the boundary. *Inverse Problems*, vol. 15, pp. 1021–1032.

**Chen, L. Y.; Chen, J. T.; Hong, H. K.; Chen, C. H.** (1995): Application of Cesàro mean and the L-curve for the deconvolution problem. *Soil Dynamics Earthquake Engineering*, vol. 14, pp. 361–373.

**Chen, K. H.; Kao, J. H.; Chen, J. T.** (2009): Regularized meshless method for antiplane piezoelectricity problems with multiple inclusions. *CMC: Computers, Materials & Continua*, vol. 9, pp. 253–279.

**Chen, C. W.; Young, D. L.; Tsai, C. C.; Murugesan, K.** (2005): The method of fundamental solutions for inverse 2D Stokes problems. *Computational Mechanics*, vol. 37, pp. 2–14.

**Cho, H. A.; Golberg, M. A.; Muleshkov, A. S.; Li, X.** (2004): Trefftz methods for time dependent partial differential equations. *CMC: Computers, Materials & Continua*, vol. 1, pp. 1–37.

**Dong, C. F.; Sun, F. Y.; Meng, B. Q.** (2007): A method of fundamental solutions for inverse heat conduction problems in an anisotropic medium. *Engineering Analysis with Boundary Elements*, vol. 31, pp. 75–82.

**Fairweather, G.; Karageorghis, A.** (1998): The method of fundamental solutions for elliptic boundary value problems. *Advances in Computational Mathematics*, vol. 9, pp. 69–95.

**Fairweather, G.; Karageorghis, A.; Martin, P. A.** (2003): The method of fundamental solutions for scattering and radiation problems. *Engineering Analysis with Boundary Elements*, vol. 27, pp. 759–769.

**Fam, G. S. A.; Rashed, Y. F.** (2009): The method of fundamental solutions applied to 3D elasticity problems using a continuous collocation scheme. *Engineering Analysis with Boundary Elements*, vol. 33, pp. 330–341.

**Gill, P. E.; Murray, W.; Wright, M. H.** (1981): *Practical Optimization*. Academic Press, London.

**Godinho, L.; Tadeu, A.; Amado Mendes, P.** (2007): Wave propagation around thin structures using the MFS. *CMC: Computers, Materials & Continua*, vol. 5, pp. 117–127.

- Golberg, M. A.; Chen, C. S.** (1999): The method of fundamental solutions for potential, Helmholtz and diffusion problems. In: M. A. Golberg (ed.) *Boundary Integral Methods: Numerical and Mathematical Aspects*, WIT Press and Computational Mechanics Publications, Boston, pp. 105–176.
- Hadamard, J.** (1923): *Lectures on Cauchy Problem in Linear Partial Differential Equations*. Yale University Press, New Haven.
- Hanke, M.** (1996): Limitations of the L-curve method in ill-posed problems. *BIT*, vol. 36, pp. 287–301.
- Hansen, P. C.** (1998): *Rank-Deficient and Discrete Ill-Posed Problems: Numerical Aspects of Linear Inversion*. SIAM, Philadelphia.
- Hon, Y. C.; Li, M.** (2008): A computational method for inverse free boundary determination problem. *International Journal for Numerical Methods in Engineering*, vol. 73, 1291–1309.
- Hon, Y. C.; Wei, T.** (2004): A fundamental solution method for inverse heat conduction problems. *Engineering Analysis with Boundary Elements*, vol. 28, pp. 489–495.
- Hon, Y. C.; Wei, T.** (2005): The method of fundamental solutions for solving multidimensional heat conduction problems. *CMES: Computer Modeling in Engineering & Sciences*, vol. 13, pp. 219–228.
- Hon, Y. C.; Wu, Z.** (2000): A numerical computation for inverse boundary determination problem. *Engineering Analysis with Boundary Elements*, vol. 24, pp. 599–606.
- Hsieh, C. K.; Kassab, A. J.** (1986): A general method for the solution of inverse heat conduction problem with partially unknown system geometries. *International Journal of Heat and Mass Transfer*, vol. 29, pp. 47–58.
- Huang, C. H.; Chao, B. H.** (1997): An inverse geometry problem for identifying irregular boundary configurations. *International Journal of Heat and Mass Transfer*, vol. 40, pp. 2045–2053.
- Huang, C. H.; Tsai, C. C.** (1998): A transient inverse two-dimensional geometry problem in estimating time-dependent irregular boundary configurations. *International Journal of Heat and Mass Transfer*, vol. 41, pp. 1707–1718.
- Jin, B. T.; Marin, L.** (2007): The method of fundamental solutions for inverse source problems associated with the steady-state heat conduction. *International Journal for Numerical Methods in Engineering*, vol. 69, pp. 1570–1589.

**Jin, B. T.; Zheng, Y.** (2006): A meshless method for some inverse problems associated with the Helmholtz equation. *Computer Methods in Applied Mechanics and Engineering*, vol. 195, pp. 2270–2280.

**Kraus, A. D.; Aziz, A.; Welty, J.** (2001): *Extended Surface Heat Transfer*. Wiley–Interscience, New York.

**Kunisch, K.; Zou, J.** (1998): Iterative choices of regularization parameters in linear inverse problems. *Inverse Problems*, vol. 14, pp. 1247–1264.

**Lesnic, D.; Berger, J. R.; Martin, P. A.** (2002): A boundary element regularization method for the boundary determination in potential corrosion damage. *Inverse Problems in Engineering*, vol. 10, pp. 163–182.

**Ling, L.; Takeuchi, T.** (2008): Boundary control for inverse Cauchy problems of the Laplace equations. *CMES: Computer Modeling in Engineering & Sciences*, vol. 29, pp. 45–54.

**Liu, C.-S.** (2008a): Solving an inverse Sturm-Liouville problem by a Lie-group method. *Boundary Value Problems*, vol. 2008, Article ID 749865.

**Liu, C.-S.** (2008b): Identifying time-dependent damping and stiffness functions by a simple and yet accurate method. *Journal of Sound and Vibration*, vol. 318, pp. 148–165.

**Liu, C.-S.** (2008c): A Lie-group shooting method for simultaneously estimating the time-dependent damping and stiffness coefficients. *CMES: Computer Modeling in Engineering & Sciences*, vol. 27, pp. 137–149.

**Liu, C.-S.** (2008d): A time-marching algorithm for solving non-linear obstacle problems with the aid of an NCP-function. *CMC: Computers, Materials & Continua*, vol. 8, pp. 53–65.

**Liu, C.-S.** (2008e): A fictitious time integration method for two-dimensional quasilinear elliptic boundary value problems. *CMES: Computer Modeling in Engineering & Sciences*, vol. 33, pp. 179–198.

**Liu, C.-S.; Atluri, S. N.** (2008a): A novel time integration method for solving a large system of non-linear algebraic equations. *CMES: Computer Modeling in Engineering & Sciences*, vol. 31, pp. 71–83.

**Liu, C.-S.; Atluri, S. N.** (2008b): A novel fictitious time integration method for solving the discretized inverse Sturm-Liouville problems, for specified eigenvalues. *CMES: Computer Modeling in Engineering & Sciences*, vol. 36, pp. 261–285.

- Liu, C.-S.; Atluri, S. N.** (2009): A fictitious time integration method for the numerical solution of the Fredholm integral equation and for numerical differentiation of noisy data, and its relation with the filter theory. *CMES: Computer Modeling in Engineering & Sciences*, vol. 41, pp. 243–261.
- Liu, C.-S.; Chang, J. R.; Chang, K. H.; Chen, Y. W.** (2008): Simultaneously estimating the time-dependent damping and stiffness coefficients with the aid of vibrational data. *CMC: Computers, Materials & Continua*, vol. 7, pp. 97–107.
- Marin, L.** (2005a): A meshless method for solving the Cauchy problem in three-dimensional elastostatics. *Computers & Mathematics with Applications*, vol. 50, pp. 73–92.
- Marin, L.** (2005b): Numerical solutions of the Cauchy problem for steady-state heat transfer in two-dimensional functionally graded materials. *International Journal of Solids and Structures*, vol. 42, pp. 4338–4351.
- Marin, L.** (2005c): A meshless method for the numerical solution of the Cauchy problem associated with three-dimensional Helmholtz-type equations. *Applied Mathematics and Computation*, vol. 165, pp. 355–374.
- Marin, L.** (2006): Numerical boundary identification for Helmholtz-type equations. *Computational Mechanics*, vol. 39, pp. 25–40.
- Marin, L.** (2008): The method of fundamental solutions for inverse problems associated with the steady-state heat conduction in the presence of sources. *CMES: Computer Modeling in Engineering & Sciences*, vol. 30, pp. 99–122.
- Marin, L.** (2009a): Boundary reconstruction in two-dimensional functionally graded materials using a regularized MFS. *CMES: Computer Modeling in Engineering & Sciences*, vol. 46, pp. 221–253.
- Marin, L.** (2009b): Regularized method of fundamental solutions for boundary identification in two-dimensional isotropic linear elasticity, submitted.
- Marin, L.; Lesnic, D.** (2003): BEM first-order regularisation method in linear elasticity for boundary identification. *Computer Methods in Applied Mechanics and Engineering*, vol. 192, pp. 2059–2071.
- Marin, L.; Lesnic, D.** (2004): The method of fundamental solutions for the Cauchy problem in two-dimensional linear elasticity. *International Journal of Solids and Structures*, vol. 41, pp. 3425–3438.

**Marin, L.; Lesnic, D.** (2005a): The method of fundamental solutions for the Cauchy problem associated with two-dimensional Helmholtz-type equations. *Computers & Structures*, vol. 83, pp. 267–278.

**Marin, L.; Lesnic, D.** (2005b): The method of fundamental solutions for inverse boundary value problems associated with the two-dimensional biharmonic equation. *Mathematical and Computers in Modelling*, vol. 42, pp. 261–278.

**Marin, L.; Karageorghis, A.; Lesnic, D.** (2009): The MFS for boundary identification in two-dimensional harmonic problems, submitted.

**Mathon, R.; Johnston, R. L.** (1977): The approximate solution of elliptic boundary value problems by fundamental solutions. *SIAM Journal on Numerical Analysis*, vol. 14, pp. 638–650.

**Mera, N. S.; Lesnic, D.** (2005): A three-dimensional boundary determination problem in potential corrosion damage. *Computational Mechanics*, vol. 36, pp. 129–138.

**Morozov, V. A.** (1966): On the solution of functional equations by the method of regularization. *Doklady Mathematics*, vol. 7, pp. 414–417.

*Numerical Algorithms Group Library Mark 21* (2007). NAG(UK) Ltd, Wilkinson House, Jordan Hill Road, Oxford, UK.

**Park, H. M.; Ku, J. H.** (2001): Shape identification for natural convection problems. *Communications in Numerical Methods in Engineering*, vol. 17, pp. 871–880.

**Peneau, S.; Jarny, Y.; Sarda, A.** (1966): Isotherm shape Identification for a two-dimensional heat conduction problem. In: H. D. Bui, M. Tanaka, M. Bonnet, H. Maigre, E. Luzzato and M. Reynier (eds.) *Inverse Problems in Engineering Mechanics*, Balkema, Rotterdam, pp. 47–53.

**Reutskiy, S. Y.** (2005): The method of fundamental solutions for eigenproblems with Laplace and biharmonic operators. *CMC: Computers, Materials & Continua*, vol. 2, pp. 177–188.

**Shigeta, T.; Young, D. L.** (2009): Method of fundamental solutions with optimal regularization techniques for the Cauchy problem of the Laplace equation with singular points. *Journal of Computational Physics*, vol. 228, pp. 1903–1915.

**Tikhonov, A. N.; Arsenin, V. Y.** (1986): *Methods for Solving Ill-Posed Problems*. Nauka, Moscow.

**Tsangaris, T.; Smyrlis, Y. S.; Karageorghis, A.** (2004): A matrix decomposition MFS algorithm for biharmonic problems in annular domains. *CMC: Computers, Materials & Continua*, vol. 1, pp. 245–258.

**Vogel, C. R.** (1996): Non-convergence of the L-curve regularization parameter selection method. *Inverse Problems*, vol. 12, pp. 535–547.

**Wahba, G.** (1977): Practical approximate solutions to linear operator equations when the data are noisy. *SIAM Journal on Numerical Analysis*, vol. 14, pp. 651–667.

**Yan, L.; Fu, C.-L.; Yang, F.-L.** (2008): The method of fundamental solutions for the inverse heat source problem. *Engineering Analysis with Boundary Elements*, vol. 32, pp. 216–222.

**Young, D. L.; Tsai, C. C.; Lin, Y. C.; Chen, C. S.** (2006): The method of fundamental solutions for eigenfrequencies of plate vibrations. *CMC: Computers, Materials & Continua*, vol. 4, pp. 1–10.

**Zeb, A.; Ingham, D. B.; Lesnic, D.** (2008): The method of fundamental solutions for a biharmonic boundary determination. *Computational Mechanics*, vol. 42, pp. 371–379.

